JAN, 2014

M.Sc. in Physics Engineering

ARDA KANDEMİR

UNIVERSITY OF GAZİANTEP

GRADUATE SCHOOL OF

NATURAL & APPLIED SCIENCES

THERMOLUMINESCENCE STUDIES OF SIM CARD CHIPS USED IN MOBILE PHONE OPERATORS IN TURKEY

M.Sc. THESIS

IN

PHYSICS ENGINEERING

BY

ARDA KANDEMİR

JANUARY 2014

Thermoluminescence Studies of SIM Card Chips Used in Mobile Phone Operators in Turkey

M.Sc. Thesis

in

Physics Engineering

University of Gaziantep

Supervisor

Asist. Prof. Dr. Hüseyin TOKTAMIŞ

by

Arda KANDEMİR

Jan 2014

REPUBLIC OF TURKEY
UNIVERSITY OF GAZİANTEP
GRADUATE SCHOOL OF NATURAL & APPLIED SCIENCES
PHYSICS ENGINEERING

Name of the thesis: Thermoluminescence Studies of SIM Card Chips Used in Mobile Phone Operators in Turkey

Name of the student: Arda KANDEMİR

Exam date: 24.01.2014

Approval of the Graduate School of Natural and Applied Sciences

Assoc. Prof. Dr. Metin BEDİR

Director

I certify that this thesis satisfies all the requirements as a thesis for the degree of Master of Science/Doctor of Philosophy.

Prof. Dr. A. Necmettin YAZICI

Head of Department

This is to certify that we have read this thesis and that in our consensus/majority opinion it is fully adequate, in scope and quality, as a thesis for the degree of Master of Science/Doctor of Philosophy.

Asist. Prof. Dr. Hüseyin TOKTAMIŞ

Supervisor

Examining Committee Members	Signature
Assoc. Prof. Dr. Metin BEDİR	.....
Asist. Prof. Dr. Hüseyin TOKTAMIŞ	.....
Asist. Prof. Dr. Abdullah KABLAN	.....

I hereby declare that all information in this document has been obtained and presented in accordance with academic rules and ethical conduct. I also declare that, as required by these rules and conduct, I have fully cited and referenced all material and results that are not original to this work.

Arda KANDEMİR

ABSTRACT

THERMOLUMINESCENCE STUDIES OF SIM CARD CHIPS USED IN MOBILE PHONE OPERATORS IN TURKEY

KANDEMİR, Arda

M.Sc. in Physics Engineering

Supervisor: Asist. Prof. Dr. Hüseyin TOKTAMIŞ

Jan 2014

81 pages

The general purpose of this study is to make necessary measurements by HARSHAW 3500 Model TLD device which is present in our "Thermoluminescence and Optically Stimulated Luminescence Laboratory" then examine SIM card chips' thermoluminescence properties and analyze these samples as suitable or not for a dosimeter. We examined three SIM card chips of different operators which are Turkcell, Avea, and Vodafone. Thermoluminescence properties of samples such as dose responses of sample, effect of heating rate on samples, reproducibility of samples and fading properties were analyzed. For irradiation processes, ^{90}Sr - ^{90}Y β radiation source was used for dose response, heating rate, reproducibility, and fading experiments. The main results from these experiments are all SIM card chips show the thermoluminescence properties, but only the Turkcell SIM card chip has good thermoluminescence properties as a dosimeter. However, that is not valid for Avea and Vodafone SIM card chips because of the bad results from experiments.

Key Words: Thermoluminescence, SIM card, chip, dosimeter

ÖZET

TÜRKİYE'DEKİ TELEFON OPERATÖRLERİN SİM KARTLARINDA KULLANILAN ÇİPLERİN TERMOLÜMİNESANS ÖZELLİKLERİNİN İNCELENMESİ

KANDEMİR, Arda

Yüksek Lisans Tezi, Fizik Müh. Bölümü

Tez Yöneticisi: Yrd. Doç. Dr. Hüseyin TOKTAMIŞ

Ocak 2014

81 sayfa

Bu çalışmanın genel amacı, "Termolüminesans ve Optik uyarmalı Lüminesans Laboratuvarımızda" mevcut olan Harshaw 3500 TLD cihazı ile gerekli ölçümleri yapıp, SIM kart çip numunelerimizin termoluminesans özelliklerini analiz ederek bu numunelerin dozimetre olarak kullanılabilir olup olmadığını incelemektir. Çalışmalarda Türkiye'deki üç farklı operatör olan Turkcell, Avea ve Vodafone'nun SIM kart çipleri kullanılmıştır. Numunelerin termolüminesans özelliklerinden; doz-yanıt, ısıtma hızı, tekrarlanabilirlik ve sönümlenme özellikleri analiz edilmiştir. Doz-yanıt, ısıtma hızı, tekrarlanabilirlik ve sönümlenme deneylerinde radyasyon işlemleri için ^{90}Sr - ^{90}Y β radyasyon kaynağı kullanılmıştır. Bu deneylerin ana sonuçları, üç operatörün SIM kart çipleri termolüminesans özelliklerine sahip, ancak sadece Turkcell SIM kart çipleri bir dozimetre olarak iyi termolüminesans özelliğine sahiptir. Fakat Avea ve Vodafone SIM kart çipleri, deneylerden elde edilen kötü sonuçlardan dolayı dozimetrik çalışmalar için elverişli değildir.

Anahtar Kelimeler: Termolüminesans, SIM kart, çip, dozimetre

To my family and relatives …

ACKNOWLEDGEMENT

I would like to thank to my supervisor Yrd. Doç. Dr. Hüseyin TOKTAMIŞ for helping and supporting me throughout the preparation of this study. Furthermore, he has checked the whole project with remarkable patience, pointing out errors which might have otherwise gone unnoticed.

I and my supervisor are grateful for financial support from the Research Fund of Gaziantep University.

I also want to thank to my whole family and Richard O'Dor for supporting and encouraging me.

TABLE OF CONTENTS

CONTENTS **Page**

LIST OF FIGURES

LIST OF TABLES

CHAPTER 1

INTRODUCTION

In today's world, energy needs and developing technologies are increasing rapidly in a proportional manner. Dosimeters are necessary equipment to measure absorbed dose in the nuclear plants, hospitals and research investigations and they are need to develop for giving the best results. There are several types of dosimeters and two of them are accidental and personal dosimeters. In the worst case scenario, we can measure the magnitude of the radiation by using accidental dosimeters which are spread around the areas of a nuclear accident or terrorist attack. In such a case, we can take the appropriate steps in these accidents by measuring the magnitude of the radiation accurately using accidental dosimeters. We can decide where the radiation is intense by comparing the radiation values or magnitudes in different regions and after these measurements we can decide correctly whether these regions are safe or not.

In addition, personnel who work in places such as oncology, radiology, laboratories, etc., should limit the radiation doses they are exposed to during while performing their duties.

Increased dosage levels may harm the health of personnel, so the value to be received from personal dosimeters which the personnel are wearing, becomes important. In these situations, we need to use appropriate personal dosimeters to ensure their health.

With the advancement of technology, humans needs are also advancing. One of the most important of these is the increasing dependence on, and increasing complexity of mobile phones. SIM cards also need to keep pace with the advancement of mobile phones.

The integrated circuit is one aspect of the 20th century which has changed almost every part of our daily life. This revolutionary product which is produced from a pot of sand, is at the heart of the smart card and changes as a normal plastic

card into a SIM card [8]. In this study, the properties of SIM card chips that are removed from the SIM cards, are investigated using thermoluminescence methods which is a part of the luminescence phenomena.

Luminescence is the emission of light from certain solids called phosphors. This emission, which does not include only black body radiation, is the release of energy stored within the solid through certain types of excitation of the electrons of the solid. This ability to store energy is important in luminescence dosimetry and is generally associated with the presence of activators. In particular, when some radiation energy is absorbed by a material, it can be re-emitted as light having a longer wavelength, according to Stokes' law. Furthermore, the wavelength of the emitted light is characteristic of the material.

The emission of light takes place a characteristic time after the absorption of the radiation and this parameter allows us to sub classify the process of luminescence. Thus we can distinguish between fluorescence in which and phosphorescence in which [2].

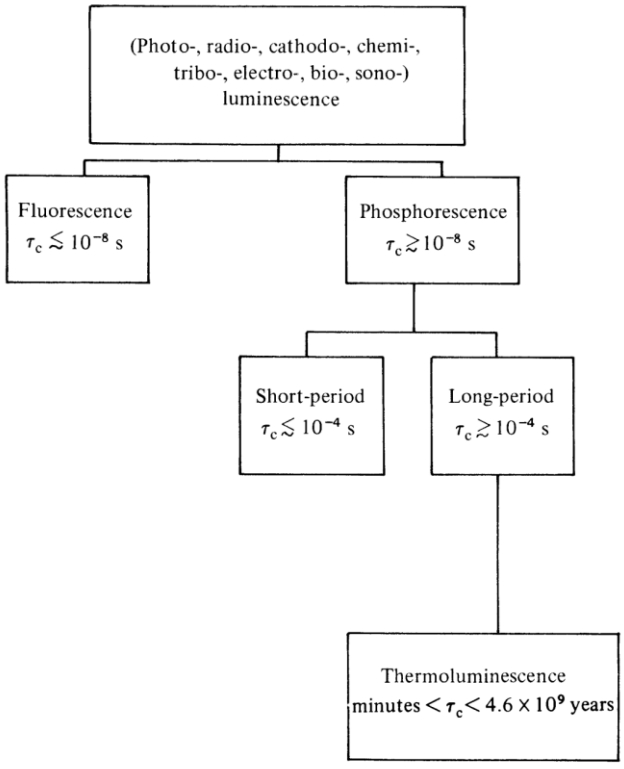

Figure1.1 The family tree of luminescence phenomena and excitation and emission

Thermoluminescence is a luminescence phenomenon of an insulator or semiconductor which can be observed when the solid is thermally stimulated. thermoluminescence should not be confused with the light spontaneously emitted from a substance when it is heated to incandescence. At higher temperatures a solid emits (infra) red radiation of which the intensity increases with increasing temperature. This is thermal or black body radiation. thermoluminescence, however, is the thermally stimulated emission of light following the previous absorption of energy from radiation. From this description the three essential ingredients necessary for the production of thermoluminescence can be deduced. Firstly, the material must be an insulator or a semiconductor, metals do not exhibit luminescent properties. Secondly, the material must absorb enough energy during exposure to radiation. A thermoluminescent material is thus a material that during exposure to ionizing radiation absorbs some energy, which is stored. The stored energy is released in the form of visible light when the material is heated. Note that thermoluminescence does not refer to thermal excitation, but to stimulation of luminescence in a sample which was excited in a different way. This means that a thermoluminescence material cannot emit light again by simply cooling the sample and reheating it another time. It should first be re-exposed to ionizing radiation before it produces light again. Thirdly, the luminescence emission is triggered by heating the material.

The storage capacity of a thermoluminescence material makes it in principle suitable for dosimetric applications. Thermoluminescence has been extensively applied in radiation dosimetry, archeological dating, geology and academic studies. Thermoluminescence glow curve analysis is also a suitable procedure applied in the characterization of the effects of impurities, natural and induced imperfections, color centers and trap distributions [1].

The goal of this thesis is to investigate SIM card chips' thermoluminescence properties and analyze whether these samples are suitable or not for a dosimeter. In this thesis, we have 5 chapters. First, background information on the experiment and technology had been given in chapter 1. In chapter 2, several subjects from chapter 1 were given more detailed explanation with literature survey. These are luminescence, thermoluminescence, chip production, dose response, heating rate effect, cycle of measurements and fading effect. In chapter 3, the materials used and the experiment methodology were detailed. All experimental results and graphs were given in

chapter 4 along with a comparison of the resulting graphs. Chapter 5 is a discussion of any conclusions that can be drawn from these experiments.

CHAPTER 2

LITERATURE SURVEY

In this chapter of the thesis, the theory of luminescence, thermoluminescence, dose response, heating rate, cycle of measurement, fading, and smart card manufacturing are described below in details.

2.1 Luminescence

Luminescence is a light phenomenon which is observed when an irradiated insulator or wide band-gap semiconductor is stimulated by an excitation energy. This excitation energy classifies the luminescence. Some luminescence phenomena and the methods of excitation are given in Table 2.1.

The description of wide band gap materials is based on a band model that corcerns absorption and storage of ionizing radiation energy and release of the stored energy as the emission of photon by thermally or optically stimulation. In the band model, absorbtion of radiation energy means creation of electron-hole pairs. The property of storing energy is due to the presence of crystal defects such as vacancies and impurities. The defects are able to capture the electrons and holes generated in the irradiation process.

A crystal defect is classified as a trap center if the defect is able to capture a charge carrier and reemit it back to the band it comes from. A crystal defect where carriers of opposite sign can be captured, resulting in an electron-hole recombination, is classified as a recombination center. For the trap center we assume that only transition between the center and the conduction band and valence band are possible. For recombination centers, we assume that only recombination of conduction electron and a valence hole is possible. Finally, an electron-hole pair is assumed initially to consist of a conduction electron and a valence hole. Exchange of charge carriers between the crystal defects are assumed to take place through the conduction and valence band [11,12]. Figure 2.1 shows the typical transitions used in simulations presented in the dissertation. During the ionizing irradiation of the

crystal, electron –hole pairs are generated by excitation of electron from the valence band to the conduction band. The excited electrons are freely moving in the crystal until they are captured by an electron trap center T_1 and T_2, or by a recombination center R. A hole generated in the valence band is captured into either a hole trap center T^h or the recombination center R. Recombinations are assumed to be accompanied by emission of photons, i.e. luminescence. However, nonradiadive recombinations are also possible.

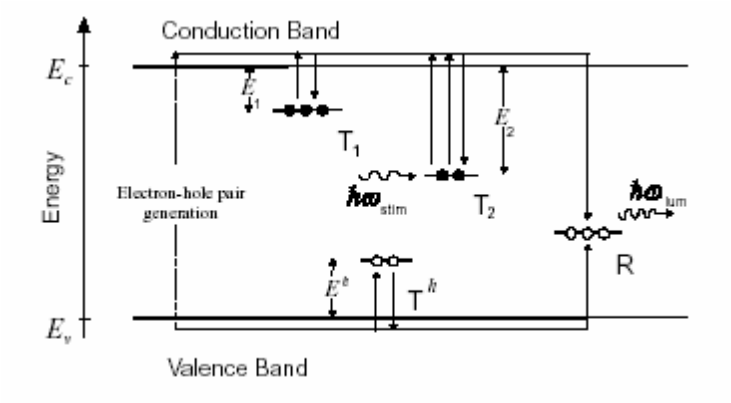

Figure 2.1 Basic concepts of irradiation, thermally and optically process between trap centers and recombination centers in a simple phenomenological band model. The transitions define whether a defect is a trap center T or a recombination center R. A recombination of an electron into a R center is assumed to be followed by photon emission[15].

By heating the crystal, captured electrons and holes can be freed thermally into the conduction or valence band and then make a transition to the radiative recombination center R. This process is termed thermoluminescence. Alternatively, external light exposure of the crystal can release captured electrons from a trap center to the conduction band from where they can recombine into the recombination center R. This phenomenon is termed optically stimulated luminescence (OSL).

The optically or thermally freed charge carriers in the conduction/valance band can be measured as electrical current when a voltage source is applied across the crystal. These measurements are termed thermally and optically stimulated conductivity (TSC, OSC), respectively.

Table 2.1 List of the luminescence phenomena and the methods of excitation.

LUMINESCENCE PHENOMENA	METHODS OF EXCITATION
Bioluminescence	Biochemical reactions
Cathodoluminescence	Electron beam
Chemiluminescence	Chemical reactions
Electroluminescence	Electric field
Photoluminescence	U.V. and infrared light
Piezoluminescence	Pressure
Triboluminescence	Friction
Radioluminescence	Ionising radiation
Sonoluminescence	Sound waves
Fluorescence Phosphorescence Thermoluminescence Lyoluminescence	Ionizing radiation, U.V. and visible light

2.2 Thermoluminescence

Thermally stimulated luminescence or thermoluminescence has been used extensively to measure nuclear radiation doses since the early 1950s [3], following the commercial availability of sufficiently sensitive and reliable photomultiplier tubes. Thermoluminescence was subsequently applied to archaeological dating in the early 1960s [4-6] and to geological dating in the beginning of the 1980s [7]. Techniques and methods used in thermoluminescence dating are reviewed by Aitken [5]. Thermoluminescence is usually observed by heating a sample at a constant rate to the finite temperature (e.g. 500^{o}C) and recording the luminescence emitted as function of temperature. The thermoluminescence signal is characterized by a so-called glow curve, with distinct peaks occurring at different temperatures, which relate to the electron traps present in the sample. Defects in the lattice structure are responsible for these traps.

A typical defect may be created by the dislocation of a negative ion, providing a negative ion vacancy that acts as an electron trap. Once trapped, an electron will eventually be evicted by thermal vibrations of the lattice. As the

temperature is raised these vibrations get stronger, and the probability of eviction increases so rapidly that within a narrow temperature range trapped electrons are quickly liberated. Some electrons then give rise to radiative recombinations with trapped holes, resulting in emission of light. A typical thermoluminescence glow curve obtained from sedimentary feldspar is shown in Figure 2.2. The temperature peaks corresponding to different electron trap depths are clearly seen.

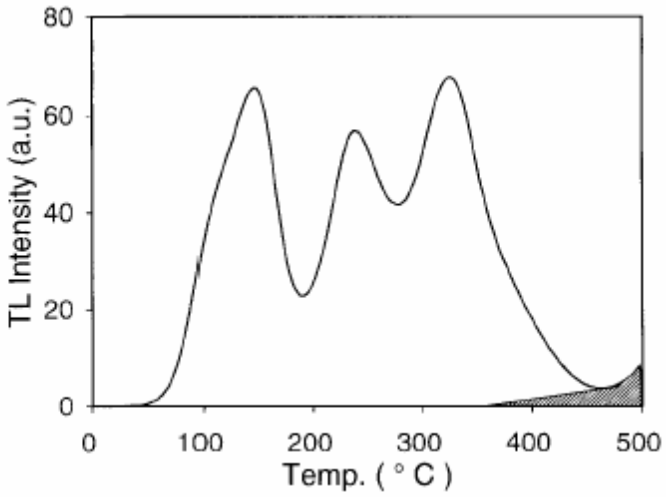

Figure 2.2 Typical thermoluminescence glow curve from a sedimentary K-feldspar sample given a beta dose of 8 Gy in addition to the natural dose (approximately 200 Gy). The 150^{o}C peak evident in this figure has been created by the recent beta dose; it is not usually evident in the natural signal as it has normally decayed away. The shaded area is the lack body radiation observed when the sample is heated a second time with no additional irradiation [15].

Although a thermoluminescence glow curve may look like a smooth continuum, it is composed of a number of overlapping peaks derived from the thermal release of electrons from traps of different stabilities. The lifetime of electrons in deep traps is longer than that of electrons in shallow traps. Normally, traps giving rise to glow peaks lower than 200^{o}C are not useful for dosimetry as electrons can be drained from these traps over a prolonged time even at environmental temperatures. Stable glow peaks suitable for dosimetry usually occur at 300^{o}C or higher. However, anomalous (i.e. unexpected) fading of high temperature glow peaks at room temperature has been observed in some feldspars. This is

explained as a quantum mechanical tunnelling effect [13]. Another complication in thermoluminescence measurements is thermal quenching. Some high temperature peaks in quartz and feldspars are subject to thermal quenching pro processes, i.e. the increased probability of non-radiative recombination at higher temperatures [14].

2.3 Models in Thermoluminescence

The aim of a mathematical analysis concerning the thermoluminescent emission of light is to achieve a satisfactory knowledge of the phenomena related to it. From a theoretical point of view, thermoluminescence is directly connected to the band structure of solids and particularly to the effects of impurities and lattice irregularities. These can be described as centers that may occur when ions of either signs move away from their original sites, thus leaving vacancy states, able to interact with free charge carriers and to trap them; alternatively, ions can diffuse in interstitial positions and break locally the ideal lattice geometry; finally, impurity ions can perturb the lattice order, because of their sizes and valences, generally different from their neighbor ones. Moreover, these extrinsic defects can interact with the intrinsic ones, and eventually either of them can aggregate in more complex configurations. From an atomic standpoint a defect can be described by means of the sign and number of charge carriers it may interact with, and the eventual existence of excited states; to such a description, a characteristic energy for each center corresponds: this may be defined as the amount of energy able, when supplied, to set the trapped charges free, thus destroying the center and restoring a situation of local order. It is feasible therefore to describe the band structure in term of valence and conduction bands, parted from each other by a forbidden gap in which the defects are represented as sites localized at different depths, below the conduction band, where free charge carriers of either sign may be trapped. Therefore, the mapping of the forbidden gap reveals quite a complex configuration, and the experimental thermoluminescence emission study can provide a satisfactory tool to get detailed information on its most meaningful parameters. These are, for each site, the characteristic energy , a frequency factor , connected to the transition frequency, and a kinetic order synthesizing the quality of the involved phenomena. The kinetic order ranges between and . The former value corresponds to a situation where a charge (electron) is supplied energy to raise in the

conduction band and, consequently, to fall to a center where it undergoes recombination with hole; the latter one stands for a situation where this phenomenon has the same probability of retrapping. Intermediate cases are likely to occur as well as contributions from non radiative events . The mathematical models based upon these definitions are consisting of convenient differential equations systems, yielding for each case, the evolution of charged carriers populations, the analytical forms of which are to be checked by means of suitable experimental data. It is therefore evident how the involved parameters are to be conveniently adjusted until a fair agreement between theory and practice is attained. The most promising tool is the observation and the recording of thermoluminescence emission, under several experimental conditions, as a function of temperature which the thermoluminescence sample is heated to, or of heating up time. For a constant heating rate, these two observations are equivalent. The plot shape depends on the physical and chemical properties of the material and on the kind of the treatment it is submitted to. However it is always a single- or multi-peak structure, as may be expected from the general equations, and a correspondence can be pointed out between a peak and an electron trap level. This is explained by considering how, at a certain temperature, the amount of thermal energy supplied reaches, for a given level, the threshold necessary to raise the relative trapped charges in the conduction band from where they can give rise to radiative recombination events. For this purpose, other centers, able to trap positive charge carriers, are involved, and they are likely to be connected to the quality of the emitted light. The analytical form for a single peak, which the overall curve is a superposition of, can fully described by means of some geometrical parameters as the peak position, its left and right widths, the ratio between them, the overall width, the height. This last one is dependent on the heating rate and increases, for given experimental conditions, with the increasing of it. These geometrical parameters can be shown to correspond to the main physical ones: the mathematical expressions can be evaluated by a convenient analytical manipulation of the involved equations. It is also to be remarked that the experimental uncertainties, obtained by means of the glow-curve plot, allow for an estimate of the physical errors related to them, and their evaluations can point out a well defined method as the fittest one [36].

2.3.1 First Order Kinetics (Randall-Wilkins Model)

In 1945, Randall and Wilkins [16] extensively used a mathematical representation for each peak in a glow curve, starting from studies on phosphorescence. Their mathematical treatment was based on the energy band model and yields the well-known first order expression. The following figure, Figure 2.3, shows the simple model used for the theoretical treatment.

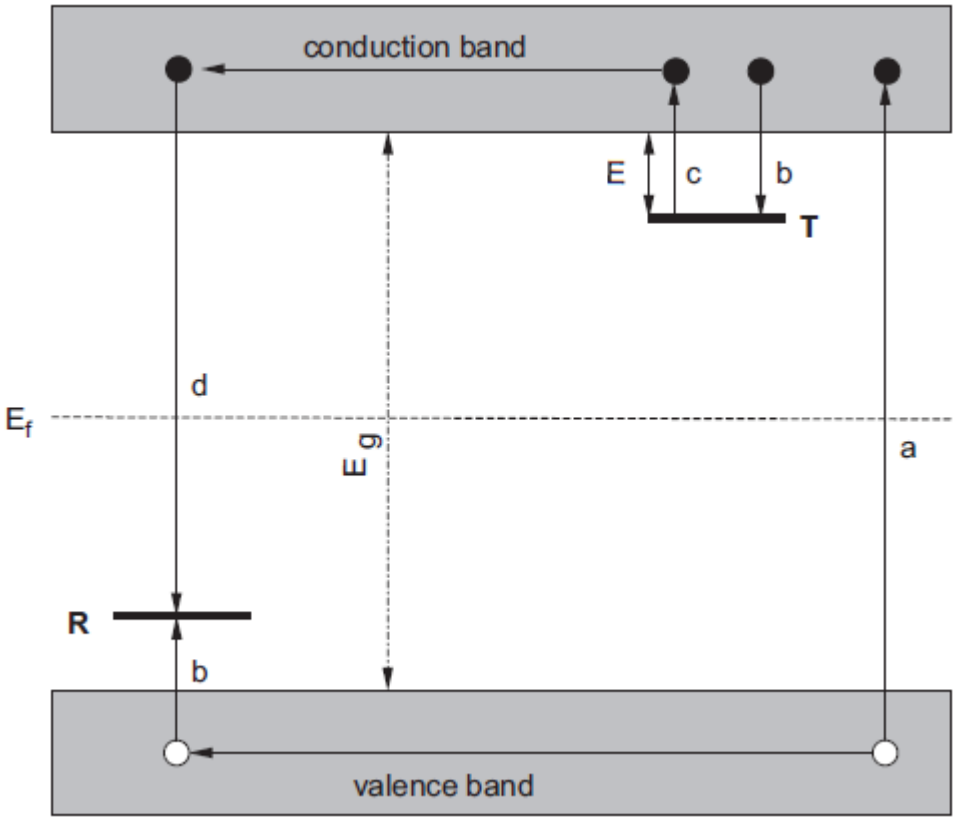

Figure 2.3 Energy band model showing the electronic transitions in a thermoluminescence material according to a simple two-level model (a) generation of electrons and holes; (b) electron and hole trapping; (c) electron release due to thermal stimulation; (d) recombination. (●) shows electrons, (○) shows holes. Level T is an electron trap, level R is a recombination centre, E_f is Fermi level [1].

Between the delocalized bands, conduction band (CB), and valence band (VB), two localized levels (metastable states) are considered, one acting as a trap, , and the other acting as a recombination center, . The distance between the trap and the bottom of the CB is called activation energy or trap depth: . This energy is the energy required to liberate a charge, i.e., an electron, which is trapped in . The

probability , per unit of time, that a trapped electron will escape from the trap, or the probability rate of escape per second, is given by the Arrhenius equation, having considered that the electrons in the trap have a Maxwellian distribution of thermal energies

—

where is the trap depth , the Boltzmann's constant, the absolute temperature , the frequency factor , depending on the frequency of the number of hits of an electron in the trap, seen as a potential well. The life time, , of the charge carrier in the metastable state at temperature , is given by

If is the number of trapped electrons in , and if the temperature is kept constant, then decreases with time according to the following expression:

—

Integrating this equation

—

one obtains

—

where is the number of trapped electrons at the initial time Assuming now the following assumptions:

- irradiation of the thermoluminescent material at a low enough temperature so that no electrons are released from the trap,
- the life time of the electrons in the conduction band is short,
- all the released charges from trap recombine in luminescent center,
- the luminescence efficiency of the recombination centers is temperature independent,
- the concentrations of traps and recombination centers are temperature independent,
- no electrons released from the trap is retrapped

According to the previous assumptions, the intensity, , of thermoluminescence in photons per second at any time during heating is proportional to the rate of recombination of holes and electrons at . If is the concentration of holes trapped at the thermoluminescence intensity can be written as

—

Here it is assumed that each recombination produces a photon and that all produced photons are detected. The rate of recombination will be proportional to the concentration of free electrons in the conduction band *n*c and the concentration of holes ,

—

with the constant the recombination probability expressed in units of volume per unit time which is assumed to be independent of the temperature.

The rate of change of the concentration of trapped electrons is equal to the rate of thermal release minus the rate of retrapping,

—

with the concentration of electron traps and the probability of retrapping . Likewise, the rate concentration of free electrons is equal to the rate of thermal release minus the rate of retrapping and the rate of recombination,

Eqns. described the charge carrier traffic in the case of release of a trapped electron from a single-electron trap and recombination in a single centre. For thermoluminescence produced by the release of holes the rate equations are similar to Eqns. . These equations form the basis of many analyses of thermoluminescence phenomena. There is no general analytical solution. To develop an analytical expression some simplifying assumptions must be made. An important assumption is at any time

This assumption is called by Chen and McKeever [17] the quasiequilibrium assumption since it requires that the free electron concentration in the conduction band is quasistationary. The trapped electrons and holes are produced in pairs during the irradiation. Charge neutrality dictates therefore

which for means that and

Since one gets from Eqns and :

Even Eqn. cannot be solved analytically without additional simplifying assumptions. Randall and Wilkins [16, 17] assumed negligible retrapping during the heating stage, i.e. they assumed . Under this assumption Eqn. can be written

Eqn. represents an exponential decay of phosphorescence. Using Eqn. in Eqn. one obtains:

Usually the temperature is raised as a linear function of time according to

with the constant heating rate and the temperature at . With using Eqn. , heating rate can be written as and introducing it into Eqn.

And the number of trapped electrons in term of

Then, using Eqn. , the intensity as a function of temperature

This expression can be evaluated by mean of numerical integration, and it yields a bell-shaped curve, as in Figure 2.4, with a maximum intensity at a characteristic temperature .

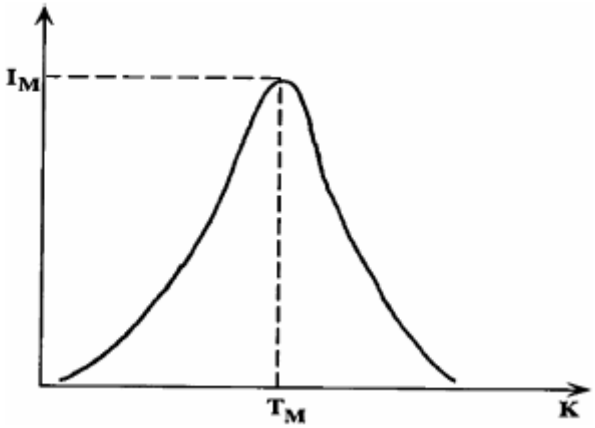

Figure 2.4 A bell shaped glow curve as a result of Randall-Wilkins model.

Some observation can be done on Eqn. :

- depends on three parameters , and ,
- has values around in the range of occurance of thermoluminescence peaks,
- is of the order of ,
- when is slightly greater than of , the argument of the second exponential function is about equal to unity and decreases with increasing temperature. is then dominated by the first exponential and increases very fast as the temperature increases. At a certain temperature, , the behaviour of the two exponential functions cancel: at this temperature the maximum temperature occurs,
- above , the decrease of the second exponential is much more rapid than the increase of the first exponential and decreases until the traps are totally emptied.

An important relationship, the so called condition at the maximum, is obtained by Eqn. by setting its first derivative equal to zero at , i.e.,

Using Eqn. it is derived

And the following expression is obtained

From Eqn. , the frequency factor is easly determined as

From Eqn. , Furetta et al. [18] have mentioned some interesting remarks :

- for a constant heating rate shifts toward higher temperatures as increases or decreases;
- for a given trap (and are constant values) shifts to higher temperatures as heating rate increases;
- is independent of .

2.3.2 Second Order Kinetics (Garlick-Gibson Model)

In 1948, Garlick and Gibson [19], in their studies on phosphorescence, considered the case when a free charge carrier has probability of either being trapped or recombining within a recombination center. The term second order kinetics is used to describe a situation in which retrapping is present. They assumed that the escaping

electron from the trap has equal probability of either being retrapped or of recombining with hole in a recombiantion centre. Garlick and Gibson considered the possibility that retrapping dominates, i.e. . Further they assume that the trap is far from saturation, i.e. and . With these assumptions, Eqn. becomes

— —— —

It is seen that now is proportional to which means a second-order reaction. With the additional assumption of equal probabilities of recombination and retrapping, , integration of Eqn. gives

—– — —— —

This is the Garlick–Gibson thermoluminescence equation for second-order kinetics. The main feature of this curve is that it is nearly symmetric, with the high temperature half of the curve slightly broader than the low temperature half. This can be understood from the consideration of the fact that in a second-order reaction significant concentrations of released electrons are retrapped before they recombine, in this way giving rise to a delay in the luminescence emission and spreading out of the emission over a wider temperature range.

2.3.3 General Order Kinetics (May-Partridge Model)

The first and second order forms of the thermoluminescence equation have been derived with the use of specific, simplifying assumptions. However, when these simplifying assumptions do not hold, the thermoluminescence peak will fit neither first nor the second order kinetics. May and Partridge [20] used for this case an empirical expression for general order thermoluminescence kinetics, namely:

— —

where has the dimension of and is defined as the general order parameter and is not necessarily or . Integration of Eqn. for yields

— — — —

where now with unit . Eqn. includes the second order case and reduces to Eqn. when . It should be noted that according to Eqn. the dimension of should be that means that the dimension changes with the order which makes it difficult to interpret physically. Still, the general order case is useful since intermediate cases can be dealt with and it smoothly goes to first and second orders when and , respectively (see Figure 2.5).

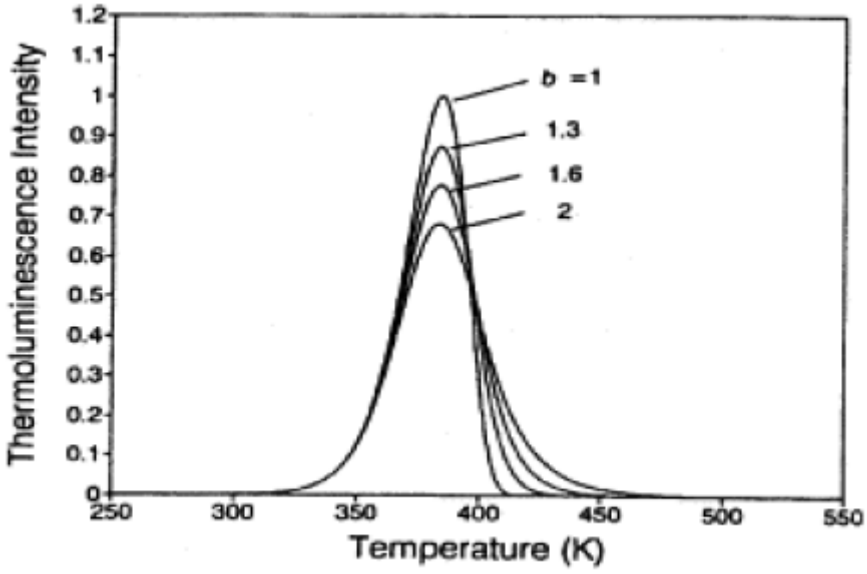

Figure 2.5 Comparison of first order , second order and intermediate order thermoluminescence peaks, with , , , and [21].

2.3.4 Advanced Models

The one trap–one centre model shows all the characteristics of the phenomenon thermoluminescence and explains the behaviour of the glow peak shape

under variation of the dose and heating rate. However, there is no existing thermoluminescence material known that accurately is described by the simple model. This does not mean that the simple model has no meaning. On the contrary, it can help us in the interpretation of many features which can be considered as variations of the one trap–one centre model. There is no room to discuss all the advanced (more realistic) models in detail. The reader is referred to the text book of Chen and McKeever [17] for a deeper and quantitative treatment. Here, only some models are very briefly mentioned in order to get some idea about the complexity of the phenomenon in a real thermoluminescence material. In general, a real thermoluminescence material will show more than one single electron trap. Not all the traps will be active in the temperature range in which the specimen is heated. A thermally disconnected trap is one which can be filled with electrons during irradiation but which has a trap depth which is much greater than the active trap such that when the specimen is heated only electrons trapped in the active trap (AT) and the shallow trap (ST) (see Figure 2.6(a)) are freed. Electrons trapped in the deeper levels are unaffected and thus this this deep electron trap (indicated in Figure 2.6(a) with DET) is said to be thermally disconnected. But its existence has a bearing on the trapping filling and eventually on the shape of the glow peak [22].

It was assumed that the trapped electrons are released during heating while the trapped holes are stable in the recombination centre. A description in which the holes are released and recombine at a centre where the electrons are stable during heating is mathematically identical. However, the situation will change if both electrons and holes are released from their traps at the same time at the same temperature interval and the holes are being thermally released from the same centres are acting as recombination sites for the thermally released electrons and vice versa (see Figure 2.6(b)). In this case Eqn. is no longer valid. New differential equations should be drafted. Analysis of this complicated kinetic model reveals a thermoluminescence glow curve which retains the simple Randall–Wilkins or Garlick–Gibson shape, depending upon the chosen values of the parameters. However, the E and s values used in and in order to obtain a fit on this complicated kinetic model need further interpretation.

Another process which might happen is a recombination without a transition of the electron into the conduction band (Figure.2.6(c)). Here the electron is thermally stimulated into an excited state from which a transition into the recombination centre is allowed. This means that the trap has to be in the proximity of a centre.

The transition probability may strongly depend on the distance between the two centres. Under certain assumptions an expression for the thermoluminescence intensity can be derived [22] which has the same form as but with replaced by a quantity related to the probability for recombination. This means that these localised transitions are governed by first-order kinetics.

Finally, Figure 2.6(d) mentions the possibility that the defect which has trapped the electron is not stable but is involved in a reaction with another defect.

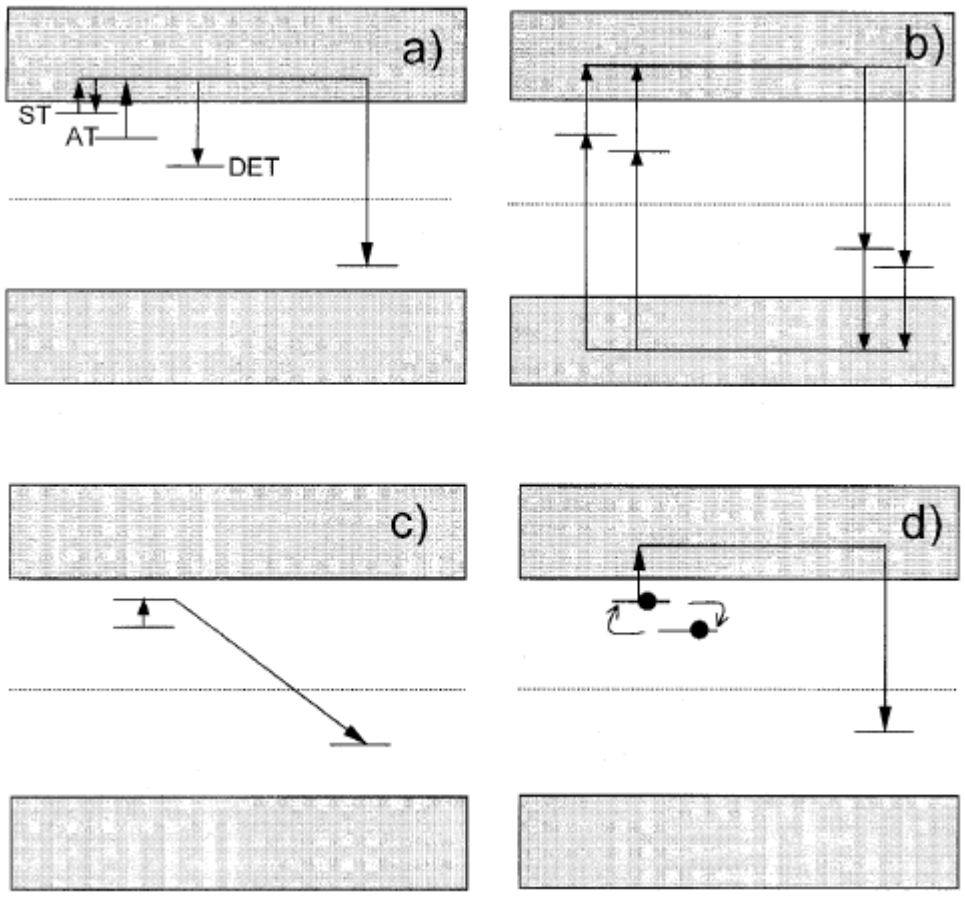

Figure 2.6 Advanced models describing the thermally stimulated release of trapped charged carriers including: (a) a shallow trap (ST), a deep electron trap (DET), and a active trap (AT); (b) two active traps and two recombination centres; (c) localised transitions; (d) defect interaction (trapping centre interacts with another defect).

The result may be that at low temperature the trap depth is changing while the trapped electron concentration is stable. At higher temperatures, electrons are involved in two processes: the escape to the conduction band and the defect reaction. Piters and Bos [23] used defect reactions incorporated into the rate equations and glow curves simulated. It appears that the simulated glow curves can be very well fitted by . It is clear that the fitting parameters do not have the simple meaning of trap depth and escape frequency.

2.4 Trapping Parameter Determination Methods

The determination of trapping parameters from thermoluminescence glow curves has been a subject of interest for half a century. There are various methods for evaluating the trapping parameters from the glow curves [16, 17, 22, 24, 25]. When one glow peak is highly isolated from the others, the experimental methods such as initial rise, variable heating rates, isothermally decay, and peak shape methods are suitable methods to determine these parameters. However in most materials, the glow curve consists of several peaks. In case of overlapping peaks, there are essentially two ways to obtain these parameters, the first one is the partial thermal cleaning method and the second one is the computer glow curve deconvolution program. In most cases, the partial thermal cleaning method can not be used to completely isolate the peak of interest without any perturbation on it. Therefore, the computer glow curve deconvolution program has become very popular method to evaluate trapping parameters from thermoluminescence glow curves in recent years [26].

2.4.1 Peak Shape Method

Evaluation of from the shape of the peak utilising parameters such as , full width at half-maximum , half width on the high temperature side of the maximum , half width on the low-temperature side of the maximum , and called the shape parameter.

The order of kinetics can be estimated by means of shape parameters. Chen [24] found that is not sensitive to changes in and , but it changes with the order of kinetics . It has been shown that the ranges of varies from for to for in case of linear heating.

The first peak shape method was developed by Grossweiner [25]; later Chen [24] modified Halperin and Braner's equations [27] for calculating values;

After determination of the activation energy and the order of kinetics, using the following expressions the frequency factor , it must be noted that this parameter called as pre-exponential factor in the general order kinetic, can be estimated for first order in and general order in kinetics respectively.

2.4.2 Isothermal Decay Method

The isothermal decay is a quite different method of analysis of the trapping parameters in which the thermoluminescence sample temperature is kept constant and the light emission can be recorded as a function of time. Generally, in the isothermal decay method, the following equation is solved for constant for the first order kinetics

where is the initial value of and

The shows that at a constant temperature , the light emission will decay exponentially with time and a plot of against will give a straight line with a slope

—

In order to find and , the experiments are carried out at two different constant temperatures and , resulting in two different slopes and . Thus the activation energy can be determined by using the following equation

——— —
— —

The isothermal decay method is not applicable to higher order kinetics. In 1979; a method has been proposed by Kathuria and Sunta [28] to calculate the order of kinetics from the isothermal decay of thermoluminescence. According to this method; if the decaying intensity from the sample is held at a constant temperature, the plot of ¯ versus gives a straight line, when the proper value of is chosen. Therefore, various values are tried and the correct one is that giving a straight line.

2.4.3 Computer Glow Curve Deconvolution (CGCD)

Computer Glow Curve Deconvolution (CGCD) is one of the most important method to determine trapping parameters from thermoluminescence glow curves. This method has the advantage over experimental methods in that they can be used in largely overlapping-peak glow curves without resorting to heat treatment In this study, a CGCD program was used to analyse the glow curve of quartz. The program was developed at the Reactor Institute at Delft, The Netherlands [29]. This program is capable of simultaneously deconvoluting as many as nine glow peaks from glow curve. Two different models were used in the computer program. In the first model, the glow curve is approximated from first order thermoluminescence kinetic by the expression,

In the second model the glow curve is approximated with general order thermoluminescence kinetics by using the expression,

where is the concentration of trapped electrons at , is the frequency factor for first-order and the pre-exponential factor for the general-order, the activation energy, the absolute temperature, Boltzmann's onstant, heating rate and the kinetic order.

The summation of overall peaks and background contribution can lead to composite glow curve formula as shown below

where is the fitted total glow curve, allows for the electronic noise contribution to the planchet and dosimeters infrared contribution to the background.

Starting from the above , the least square minimisation procedure and also FOM (Figure of Merit) was used to judge the fitting results as to whether they are good or not. i.e.

where is the i-th experimental points (total data points) , is the i-th fitted points, and is the integrated area of the fitted glow curve.

From many experiences [30-31], it can be said that if the values of the FOM are between and the fits is good, and the fits is fair, and bigger than fit is bad.

To have a graphic representation of the agreement between the experimental and fitted glow curves, the computer program also plots the function,

which is a normal variable with an expected value and where

2.4.4 Initial Rise Method

The simplest, and most generally applicable method for evaluating the activation energy of a single thermoluminescence peak is the initial rise method. The basic premise upon this method which is based is that at the low temperature end of the peak, all the relevant occupancies of the states, the trap, the recombination center and, in some cases, other interactive states can be considered as being approximately constant.

The rise of the measured intensity as a function of temperature in this region is, therefore, very close to exponential, thus

where the constant includes all the dependencies on the other parameters and occupancies, is the activation energy , is the Boltzmann's constant and is the temperature . Plotting against a linear plot is obtained with slope equal to . Hence it is possible to evaluate without any knowledge of the frequency factor by means of equation

Once the value of was determined, the frequency factor was obtained from the equation

___ —

where is the temperature at the maximum intensity. This method can only be used when the glow peak is well defined and clearly seperated from the other peaks.

2.4.5 Heating Rate Method

Another important method is various heating rates for the determination of activation energies. If a sample is heated at two different linear heating rates and the peak temperatures will be different. Equation (2.40) can therefore, be written for each heating rate and dividing the equation for (and) by the equation for (and) and rearranging, one gets an explicit equation for the calculation of

_____ — —

The major advantage of the heating rate method is that it only requires data to be taken at a peak maximum which, in case of a large peak surrounded by smaller satellites, can be reasonably accurately determined from the glow curve. Furthermore the calculation of *E* is not affected by problems due to thermal quenching, as with the initial rise method.

When various heating rates for the first order kinetics are used, the following expression is obtained:

— – —

A plot of versus should yield a straight line with a slope , then is found. Additionally, extrapolating to , a value for is obtained from which can be calculated by inserting the value of found from

the slope. This method of various heating rates are applicable for general order kinetics which includes the second order case. For the general order case, one can plot versus , whose slope is equal to .

2.5 Dose Response

Dose can be defined either as the accumulated amount of irradiation incident on the sample during any period at low temperature or the total amount absorbed prior to the heating [9]. There are two types of nonlinear dose dependence in dose response studies. These are sublinear and supralinear. The supralinearity is the increase in the derivative of the dose dependence function [10]. The measured thermoluminescence signal by , be it either the maximum intensity or the total area under the peak, as a function of the dose . The derivative of this function at any point is , and an increase of the derivative at a certain point is expressed by stating that is positive. Thus represents ranges of supralinearity; characterizes ranges of sublinearity, and of course signifies a range of linearity [9].

2.6 Heating Rate Effect

In thermoluminescence measurements, heating rate is a fundamental experimental variable [30]. The dependence of thermoluminescence on the heating rate may be utilized for determining trap parameters of studied material. Typically, with increasing heating rate (β) the thermoluminescence glow curve is shifted towards higher temperatures. As a consequence, one should expect decrease of the area (the total number of emitted photons) at higher heating rates [31]. In addition, it plays a critical role in deciding the time required to record the thermoluminescence glow curves because thousands of dosimeters have to be processed in a short time when personnel monitoring is carried out using thermoluminescence dosimeters. This is also important because higher heating rate not only increases the glow peak height but also records the glow curves faster, which forms the basis of thermoluminescence dosimetry in large scale personnel monitoring. In literature there are large numbers of reports that demonstrate that for a constant dose, the glow peak height decreases with increase in heating rate [32].

2.7 Cycle of Measurements (Reproducibility)

It is obvious that the most desirable feature is reproducibility; one hopes that repeating a measurement several times would yield the same results. It sometimes happens, however, that a cycle of excitation and heating changes the sample in such a way that the sensitivity to the next excitation changes. Such a change may be detrimental to the basic analysis of the measured effect; however, following such a change of sensitivity in detail may add information about the studied sample. The same can be said about the applications in which one tries to evaluate the dose imparted on the sample; changes in sensitivity may disrupt this goal [33]. A standard deviation of or less is the index for a good reproducibility [34].

2.8 Fading Effect

A good TLD material is able to store the information (trapped charge carriers) without loss. The release of electrons and holes from their traps and consequently their recombination is a statistical phenomenon, the probability of which is a function of temperature. The probability:

—

(where p is the transition probability, S is the vibrational factor characteristic of the centre, E is the activation energy, k is the Boltzmann's constant, and T is the absolute temperature) that the electrons escape before the read-out and thus the peak intensity will decrease in course of time at a rate governed by the temperature at which the sample is stored after the irradiation and by the rate parameters and . The signal is said to have faded. In other words, reduction of the thermoluminescence signal because of the electron escape before the read-out. As is well known, the unintentional loss of the latent information is called fading. Temperature is normally responsible for this loss, but other quantities such as light can greatly influence the latent information in the thermoluminescence material [35].

2.9 Smart Card

There are two processes to produce smart card. First is the production of the wafer. Second is fabrication of the chip by using a wafer.

2.9.1 Production of Wafer

There are 4 main steps to produce a wafer. These are:

- Growth Technique
- Grinding and Dicing
- Lapping and Etching
- Polishing and Cleaning

2.9.1.1 Growth Technique

The common growth technique is the Czochralski-technique which is a method to pull a monocrystal with the same crystallographic orientation of a small monocrystalline seed crystal out of melted silicon. First, electronic-grade polysilicon nuggets optionally together with dopants are melted in a quartz crucible at a temperature in an inert gas atmosphere. The quartz crucible sits inside a graphite container which – due to its high heat conductivity – homogeneously transfers the heat from the surrounding heater to the quartz crucible. The silicon melt temperature is kept constant roughly above the silicon melting point. A monocrystalline silicon seed crystal with the desired crystal orientation (e. g. , or) is immersed into the melt and acts as a starting point for the crystal formation supported by the heat transfer from the melt to the already grown crystal. The seed crystal is slowly (few) pulled out of the melt, where the pull speed determines the crystal diameter. During crystal growth, the crystal as well as the crucible counter-rotate in order to improve the homogeneity of the crystal and its dopant concentration. Before the crystal growth is finished, a continuous increase of the pull speed reduces the crystal diameter towards zero. This helps prevent thermal stress in the ingot which could happen by an abrupt lifting out of the melt and could destroy the crystal.

2.9.1.2 Grinding and Dicing

The ingots grown with the Czochralski or float-zone technique are ground to the desired diameter and cut into shorter workable cylinders with e. g. a band saw

and ground to a certain diameter. An orientation flat is added to indicate the crystal orientation, while wafers with an 8 inch diameter and above use a single notch to convey wafer orientation, independent from the doping type. Two common techniques are applied for wafer dicing: Inside hole saw and wire saw. For Inside Hole Saw (Annular Saw), the wafers are sawed inside a circular blade whose cutting edge is filled with diamond splinters. After sawing, the wafer surfaces are already relatively flat and smooth, so the subsequent lapping of the surfaces takes less time and effort. However, only one wafer per annular saw can be cut at the same time, so this technique has a comparably low throughput which makes the wafers more expensive compared to wafers cut by a wire saw. In order to increase throughout, wire saws with many parallel wires are used which cut many wafers at once. A long high-grade steel wire with a diameter of is wrapped around rotating rollers with hundreds of equidistant grooves at a speed of typically . The mounted silicon cylinder is drained into the wire grid and thus cut into single wafers.

The wire is either coated with diamond splinters or wetted with a suspension of abrasive particles such as diamonds or silicon carbide grains, and a carrier (glycol or oil). The main advantage of this sawing method is that hundreds of wafers can be cut at a time with one wire. However, the attained wafer surface is less smooth and more bumpy as compared to wafers cut by an annular saw, so the subsequent lapping takes more time.

2.9.1.3 Lapping and Etching

After dicing, the wafers are lapped on both sides in order to remove the surface silicon which has been cracked or otherwise damaged by the slicing process (e. g. grooves by the wire saw) and thinned to the desired wafer thickness. Several wafers at a time are lapped in between two counter-rotating pads by a slurry consisting of e. g. or abrasive grains with a defined size distribution. Wafer dicing and lapping degrade the silicon surface crystal structure, so subsequently the wafers are etched in either or based etchants in order to remove the damaged surface.

2.9.1.4 Polishing and Cleaning

After etching, both wafer surfaces appear like the rear side of finished single-side polished wafer. In order to attain the super-flat, mirrored surface with a remaining roughness on atomic scale, the wafers have to be polished. Wafer polishing is a multi-step process using an ultra-fine slurry with sized grains consisting of e. g. , or which, combined with pressure, erode and mechanically and chemically smoothen the wafer surface between two rotating pads. Finally, the wafers are cleaned with ultra-pure chemicals in order to remove the polishing agents thereby making them residual-free [39].

2.9.2 Fabrication of Chip

The fabrication of the card involves a number of processes as shown in Figure 2.7. The first part of the process is to manufacture a substrate which contains the chip. This is often called a COB (Chip On Board) and consists of a glass epoxy connector board on which the chip is bonded to the connectors. There are three technologies available for this process, wire bonding, flip chip processing and tape automated bonding (TAB). In each case the semiconductor wafer manufactured by the semiconductor supplier is diced into individual chips . This may be done by scribing with a diamond tipped point and then pressure rolling the wafers so that it fractures along the scribe lines. More commonly the die are separated from the wafer by the use of a diamond saw. A mylar sheet is stuck to the back of the wafer so that following separation the dice remain attached to the mylar film.

Wire bonding is the most commonly used technique in the manufacture of smart cards. Here a gold or aluminum wire is bonded to the pads on the chip using ultrasonic or thermo compression bonding. Thermo compression bonding requires the substrate to be maintained at between and . The temperature at the bonding interface can reach 3 . To alleviate these problems thermo sonic bonding is often used which is a combination of the two processes but which operate at lower temperatures. The die mounting and wire bonding processes involve a large number of operations and are therefore quite expensive. Because in general only or wires are bonded for smart card applications this approach is acceptable. However in the semiconductor industry generally two other techniques are used, the flip chip process and tape automated bonding. In both cases gold bumps are formed on the die. In flip chip processing the dice are placed face down on the

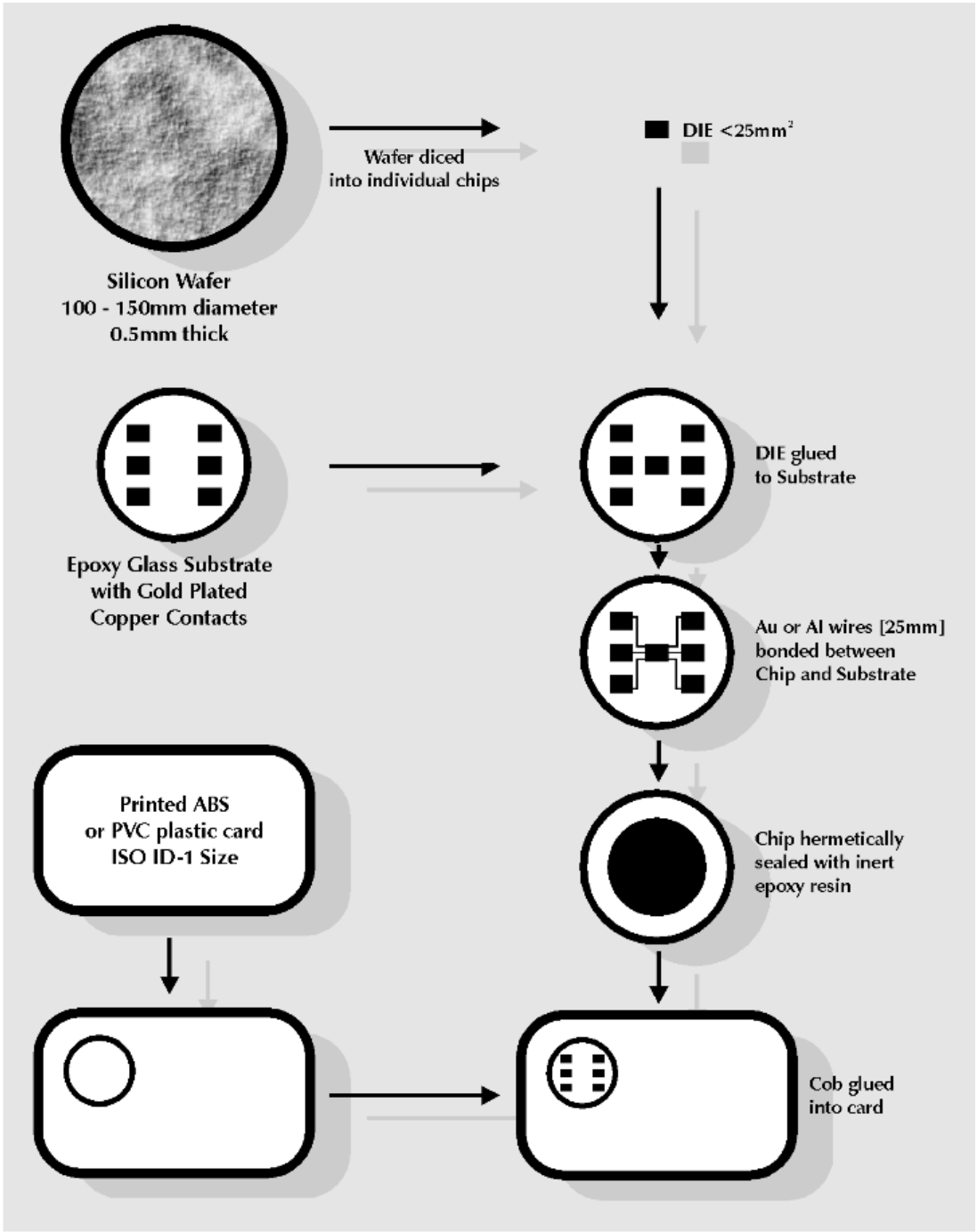

Figure 2.7 Smart Card fabrication process

substrate and bonding is effected by solder reflow. With tape automated bonding the dice are attached by thermo compression to copper leads supported on a flexible tape similar to a film. The finished substrate is hermetically sealed with an inert material such as epoxy resin. The complete micro module is then glued into the card which contains the appropriately sized hole [37].

On the way to the final product for the customer there are several steps in card production. First there is the manufacturing of the card body - which includes making of the plastic, printing, and adding additional elements, such as the magnetic stripe. This is followed by embedding the smart card module, which itself went through the steps of test completion and initialization. And finally, optical and electrical personalization transforms the smart card to an individual one [38].

2.10 Thermoluminescence Properties of Smart Card Chip

Both radiation accidents and radiological terrorism could be evaluated with the help of daily-use materials that can act as potential dosimeters. A daily-use material, such as SIM card chips exhibit a reasonable sensitivity to radiation based on its thermoluminescence (TL) property. The thermoluminescence emission features of SIM card chip allow us to think that could be used for dose reconstruction in areas affected by a nuclear accident or large-scale incidents involving population groups where conventional dosimetric systems may not be at hand.

The main advantage of SIM card chips as a personal dosimeter is that almost every individual at present possesses a SIM card chips either in the form of health-care identity cards or as a phone card. In case of accidental radiation, SIM card chips can be collected and used for the assessment of radiation doses to individuals. The radiation dose responses of this material can be measured using luminescence. The signal is stable at ambient temperature and linear with radiation dose from
up to . Such properties render these forms of chip-cards suitable for a non-invasive reconstruction of doses for individuals in case of radiation accidents [40-43].

CHAPTER 3

EXPERIMENT

The equipments, materials and experimental procedures utilized in this study are described below in details.

3.1 Equipment

3.1.1 ^{90}Sr - ^{90}Y β Radiation Source

The ^{90}Sr - ^{90}Y β radiation source is located in our TL and OSL laboratory. The irradiation equipment is an additional part of the 9010 optical dating system which is interfaced to a PC using a serial RS-232 port to control the irradiation duration. The samples were irradiated at room temperature and our β radiation source irradiated materials with .

Figure 3.1 ^{90}Sr - ^{90}Y β radiation source and computer.

3.1.2 Harshaw 3500 TL Reader and Peak Analyzer

The Harshaw 3500 includes a sample drawer for a single element TLD dosimeter, a linear, programmable heating system and a cooled photomultiplier tube with associated electronics to measure the thermoluminescence light output [44]. It is the device where the irradiated materials are heated and the intensity of the light output measured. Using the software program Winrems, we can set the starting and ending temperatures of the heating process, and the temperature increments. Search Response Database (RSP) is used to view the results. Temperature settings are made with the Time Temperature Profile (TTP). The glow curves were obtained by using a Harshaw QS 3500 Manual type thermoluminescence reader interfaced to a PC, where the thermoluminescence signals were analyzed. The basic block diagram of reader is shown in Figure 3.3.

Figure 3.2 Harshaw 3500 TL Reader.

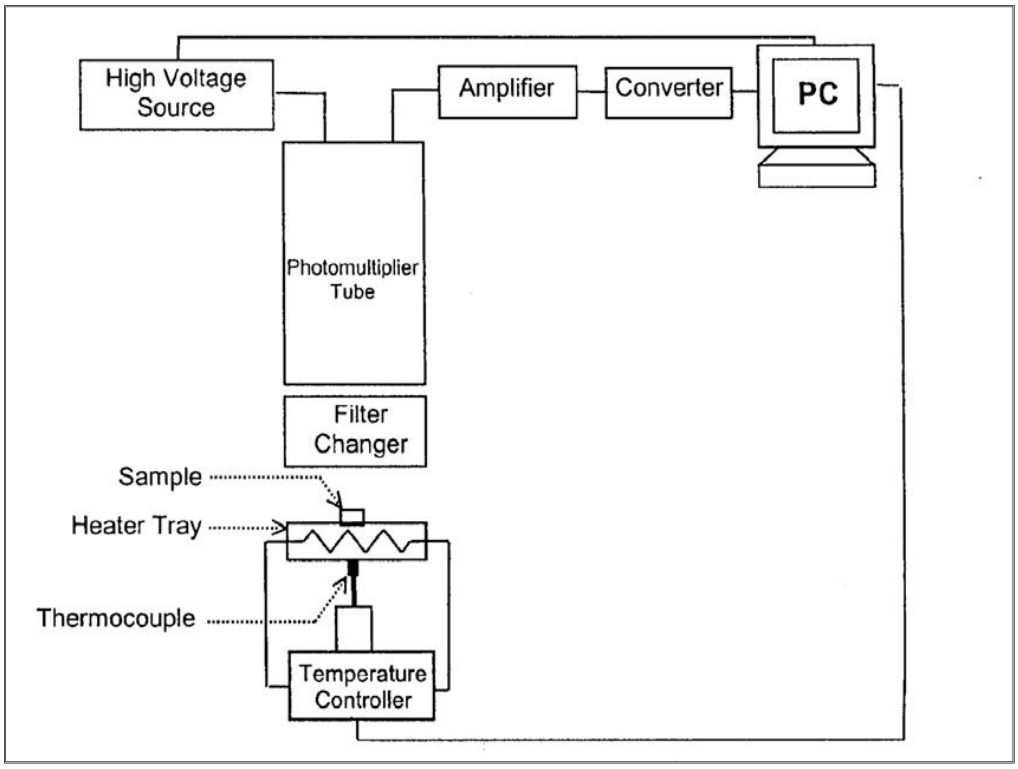

Figure 3.3. Basic block diagram of TL reader.

3.1.4 Fading Box

The samples are placed in a box in a completely dark environment to protect from light contamination. This box is called a fading box. We used a match box as a fading box in the fading processes.

Figure 3.4. Fading box and fading cupboard

3.2 Materials

The materials which are used in the experiments are SIM card chips from the three different operators in Turkey. These are:

- Avea
- Turkcell
- Vodafone

The size of the SIM cards is equal and . The size of the core of the SIM card chips is . This core material of a chip extracted from a SIM card, is commonly . Chip composition can be detected by X-Ray Diffraction (XRD) method. It was concluded, by survey methods, that all the sample SIM card chips are made with [40]. In this study, the SIM card chip samples were extracted as dust and bulk according to the extraction. If the extraction is easy, the sample extracts as bulk otherwise the sample extracts as dust. That is why, Avea SIM card chip sample was extracted as dust.

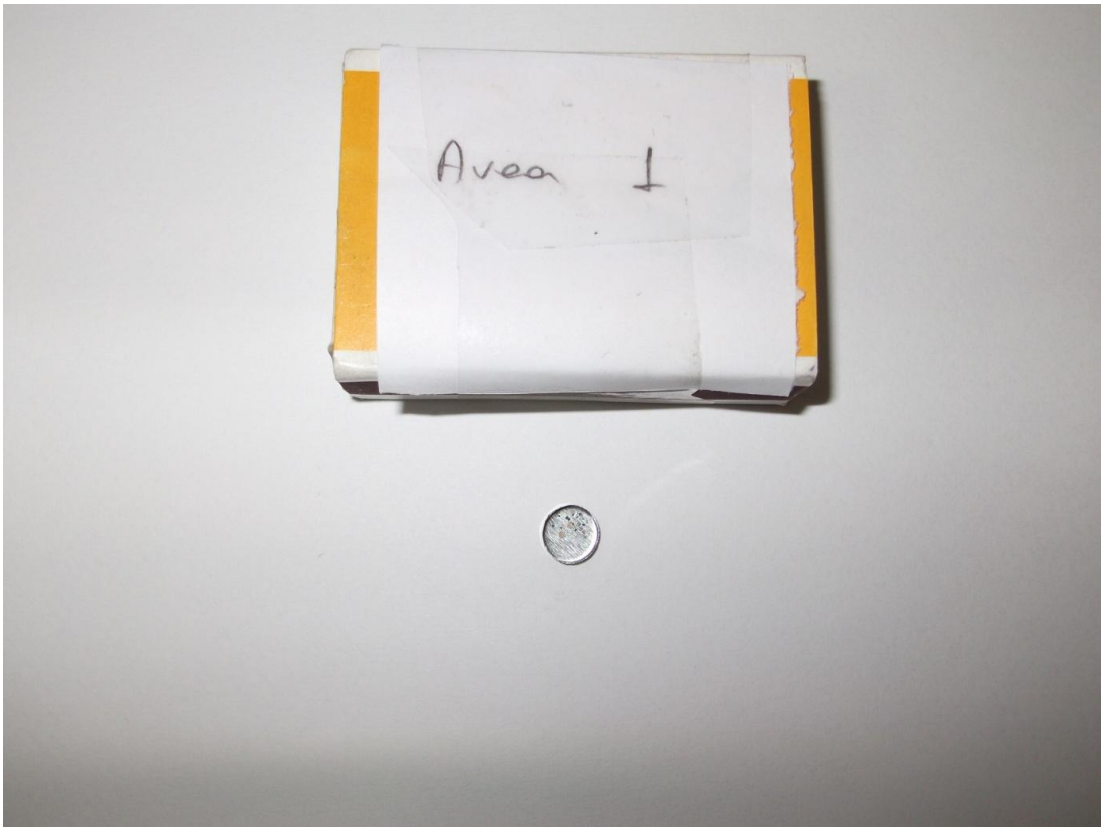

Figure 3.5 Avea SIM card chip (Dust).

Figure 3.6 Turkcell SIM card chip.

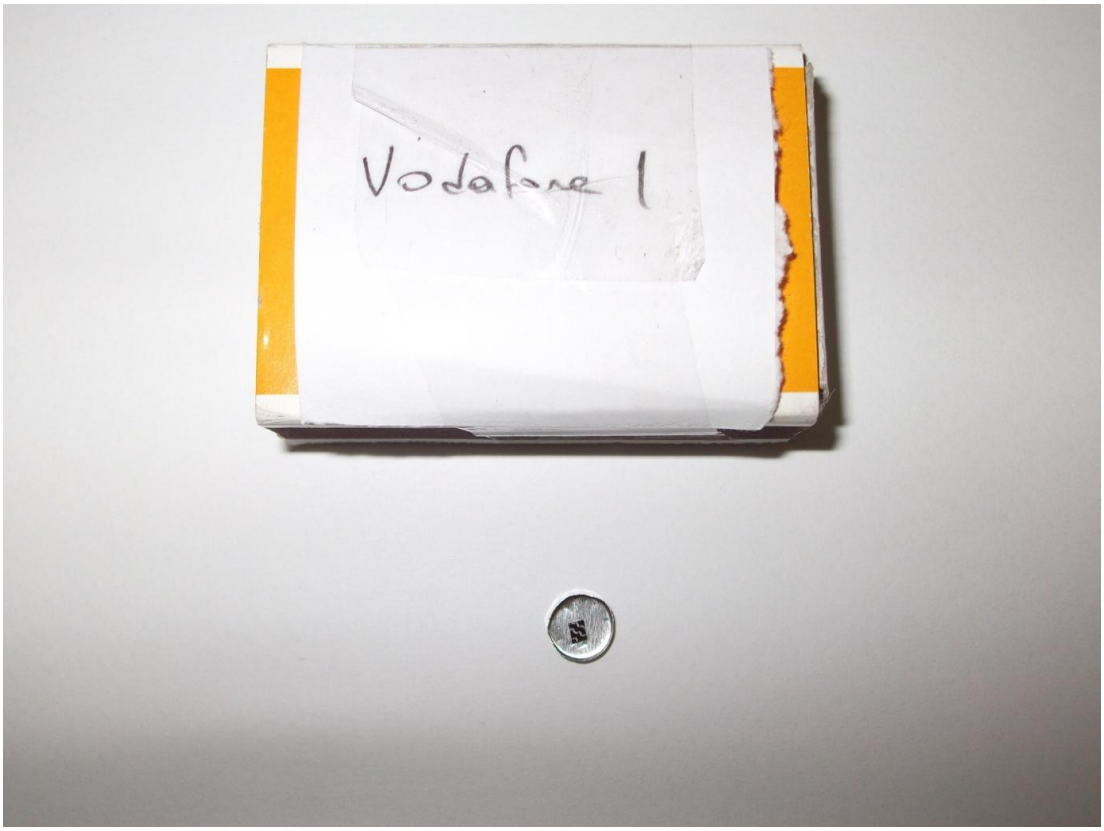

Figure 3.7 Vodafone SIM card chip.

3.3 Procedure

3.3.1 Extraction of Chip

First, the samples (SIM card chips) need to be removed from SIM cards. For this process, the SIM cards are cut with a box cutter then carefully divided into two pieces to extract the chips from SIM cards. After the extraction of the chips, they are put into the sample containers. If the extraction process is too difficult, the samples are turned to dust and the resulting dust samples are collected into the sample containers.

3.3.2 Natural Dose

The purpose of this experiment is the evacuation of the traps (resetting process) which are located in the forbidden gap of the SIM card chips. In this experiment, the samples cannot be subjected to any radiation. The samples are heated up from to in per second increments in Harshaw 3500 TLD Reader. This heating process evacuates the traps and leaves them empty of all residual thermoluminescence radiation.

3.3.3 Dose Response

The purpose of the Dose Response process is to measure the thermoluminescence light intensity of sample for different radiation values. First the sample is irradiated by the ^{90}Sr-^{90}Y β radiation source about for the radiation process. After the radiation process, sample is put into the Harshaw 3500 TLD reader for reading. The TLD reader heats the sample from to with heating rate of and analyzes the thermoluminescence light output from the sample and the glow curve of the sample. Then the sample's traps need to be emptied for another irradiation process and to take background emission to subtract from the total emission . Therefore we use the TLD reader again and it heats the sample from to in per second increments for the resetting process. Each process is repeated for 4.8, 9.6, 19.2, 38.4, 76.8, 153.6, 307.2, 614.4, 1228.8, 2457.6 minutes radiation dose.

3.3.4 Heating Rate Effect

This is similar to the Dose Response case. The differences are constant radiation dose and varying heating rate . First the sample is irradiated by the

radiation source about for radiation process. After the radiation process, the sample is put into the TLD reader for reading. The TLD reader heats the sample from to with heating rate of and analyzes the thermoluminescence light output from the sample. Then the sample's traps are emptied, using the TLD reader resetting procedure outlined previously, then irradiate it again using a constant . After each radiation process has been completed, the heating rate was increased to , 4 , 8 , , , and for reading and resetting analysis.

3.3.5 Cycle Measurements

In this case, the radiation dose and heating rate are held constant. was used for the radiation process and for reading and resetting analysis. First the sample is put into the radiation source, and after the radiation process has been completed it is put into the TLD reader for reading. The TLD reader heats the sample from to with heating rate of and analyzes the thermoluminescence light output from the sample. Then the sample's traps are emptied, the process is repeated eight times, and the results are checked for consistency.

3.3.6 Fading Effect

First the sample is irradiated by the radiation source. We use for radiation process. After the radiation process has been completed, the samples are placed in a box in a completely dark environment to protect from light contamination and held for different time intervals. First, the sample is kept for 1 hour in the dark. After that waiting process, our sample is put into TLD reader for reading from to in with heating rate of . Then, the sample's traps are emptied and the process is repeated, keeping the sample in the dark for 2, 4, 8, 16, 32, 64, 128, 256, 512, and 1024 hours.

CHAPTER 4

EXPERIMENTAL RESULTS AND DISCUSSIONS

In this chapter, we examined the experimental results under three cases which are:

- Dose Response
- Heating Rate Effect
- Cycle of Measurements
- Fading Effect

4.1 Dose Response

The glow curves of samples were examined by using different doses in this part of the experiments.

4.1.1 Variation of Glow Curve

Glow curve is the plot of the thermoluminescence intensity as a function of the temperature of sample during read out. The glow curve variation of chips that extracted from SIM card were examined for:

- Turkcell
- Avea
- Vodafone

Figure 4.1 shows the variation of glow curve as a function of doses for the (a) Turkcell sample, (b) Avea sample, and (c) Vodafone sample. In Figure 4.1 (a), the shape of glow curves do not change by using different doses. There are no extra peaks and peaks increase in same proportion. In Figure 4.1 (b), the shape of glow curves do not significant change by using different doses except dose

experiment. There are extra peaks and peaks are not increased in same proportion. In addition, there is an observation that the dose increases, the area under curve of low temperature peaks increase. At the higher doses, the structure of traps and the number of traps are being changed. So this sample is not suitable for precision radiation intensity measurements based on the glow curve.

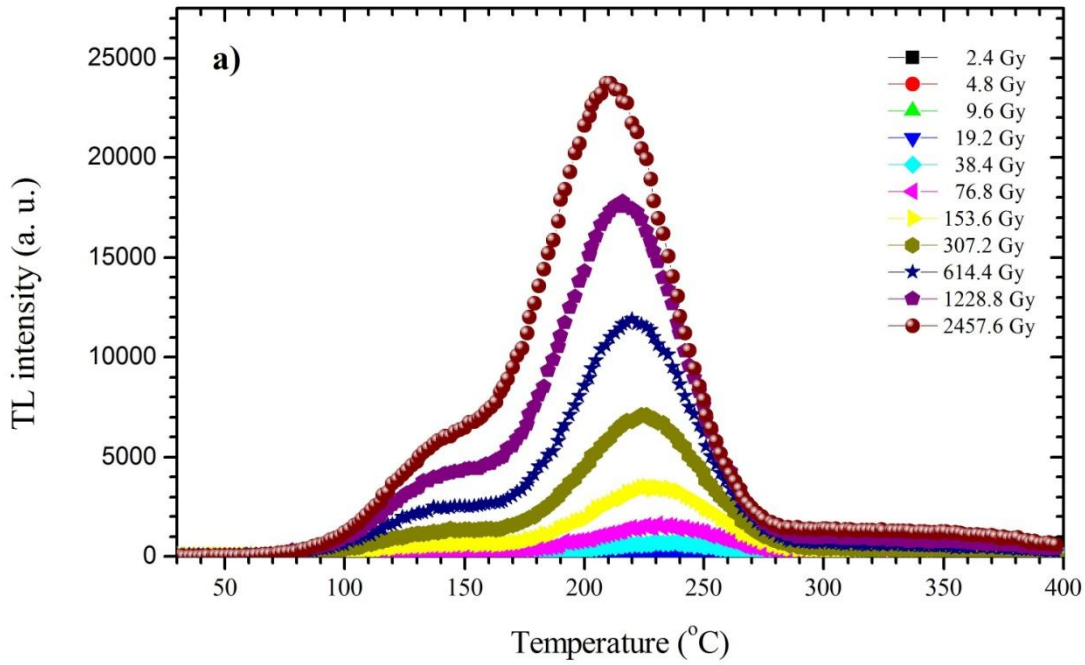

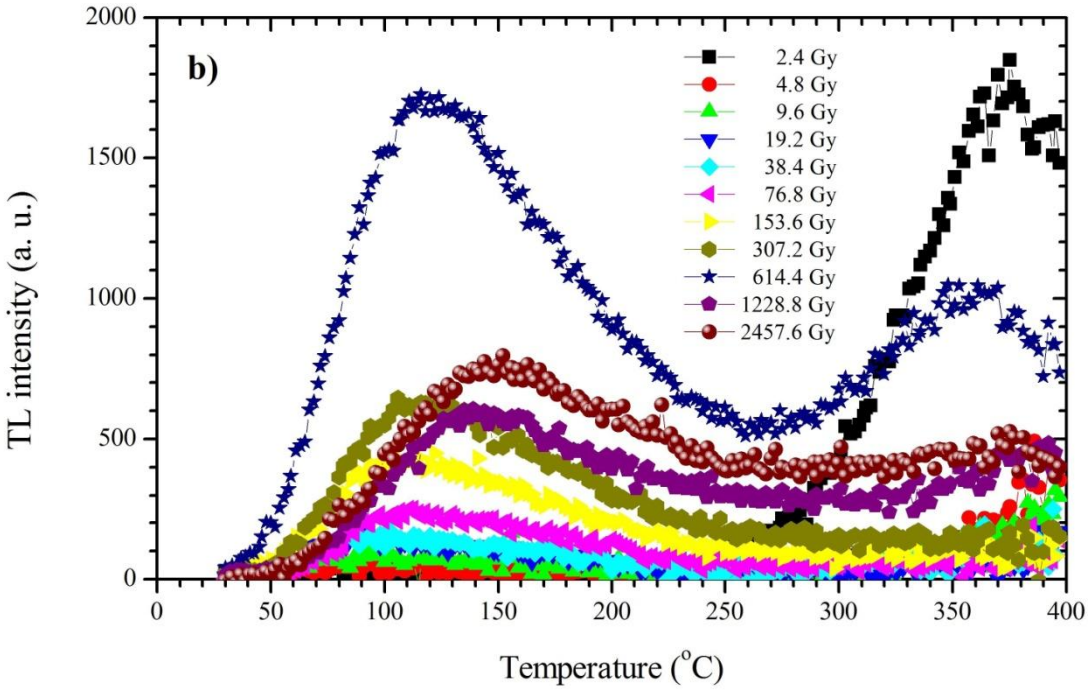

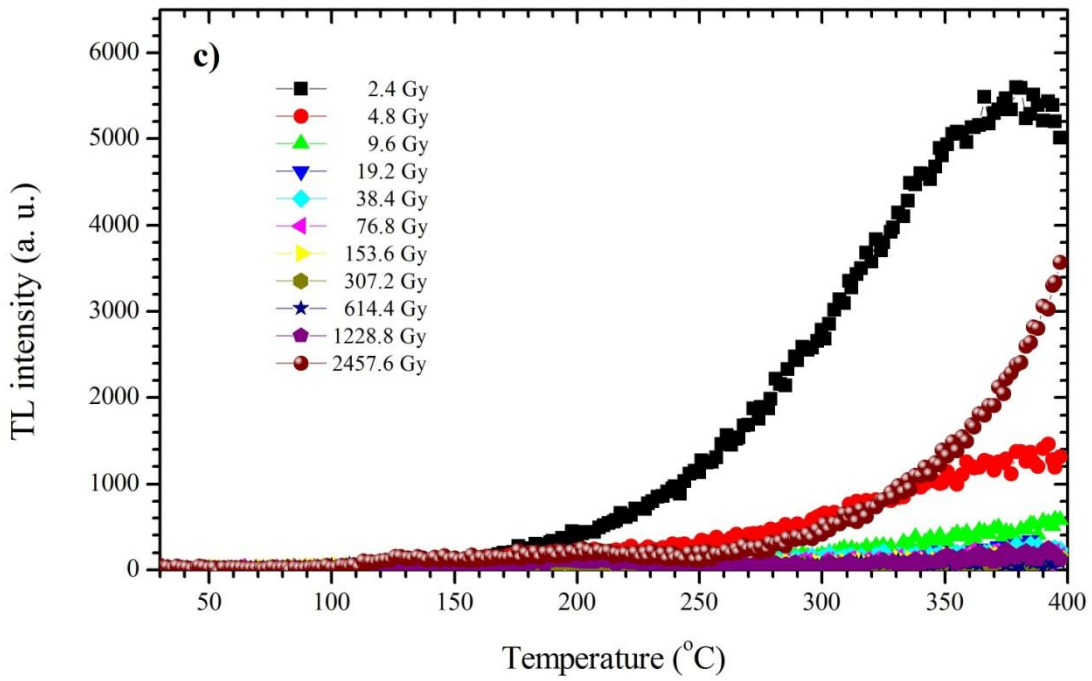

Figure 4.1 Variations of the glow curve for different doses for the (a) Turkcell sample, (b) Avea sample, (c) Vodafone sample.

In Figure 4.1 (c), there are not any peaks in the glow curve except for taking information about sample. This sample is also not suitable for precision radiation intensity measurements based on the glow curve.

4.1.2 Variation of Peak Temperature

In this part of the experiment, the effects of the different doses on the peak temperatures of thermoluminescence intensity were examined.

Figure 4.2 shows the variation of peak temperature as a function of doses for the (a) Turkcell sample, (b) Avea sample, and (c) Vodafone sample. In Figure 4.2 (a), if the dose increases, the peak temperature decreases because the structure of traps may change with increasing dose. This change occurs in the forbidden band gap. In this graph we used a logarithmic scale. The peak temperature shifts from to . In Figure 4.2 (b), the peak temperature line decreases sharply at first with increasing dose, but after , the peak temperature line increases with increasing dose. In this graph we used a logarithmic scale as well. In Figure 4.2 (c), for the low dose region, there is no change in the peak temperature when we increase the dose. The peak temperature decreases with increasing dose from to .

After there are fluctuations when the dose is increased and in the high dose region, there is no change in the peak temperature the dose is increased. This graph is drawn also on logarithmic scale.

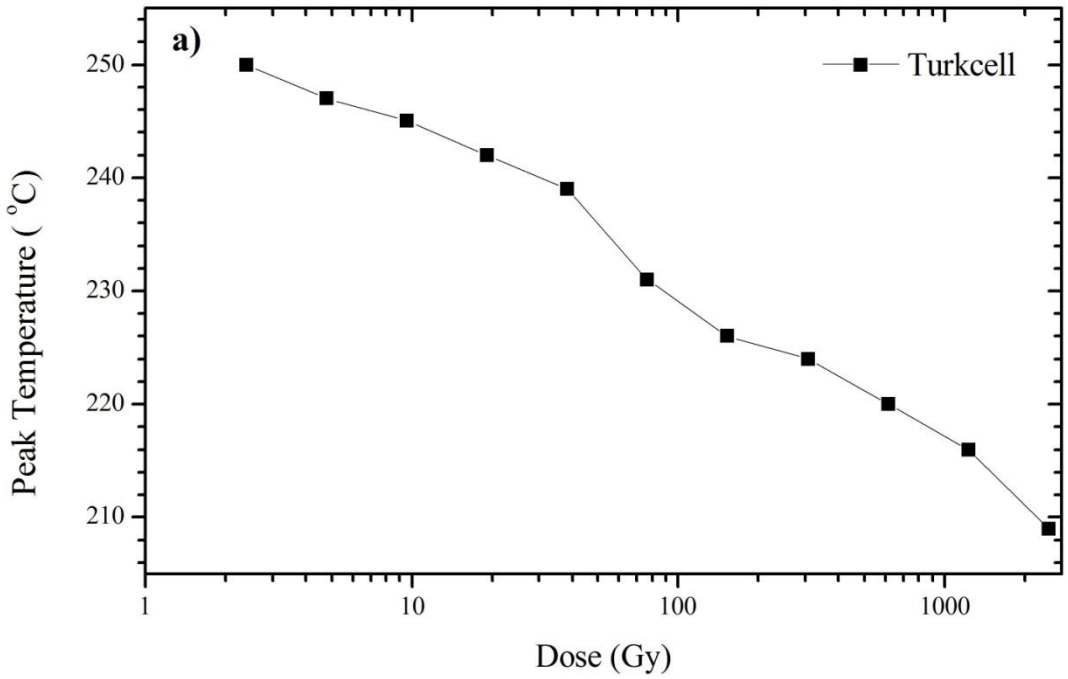

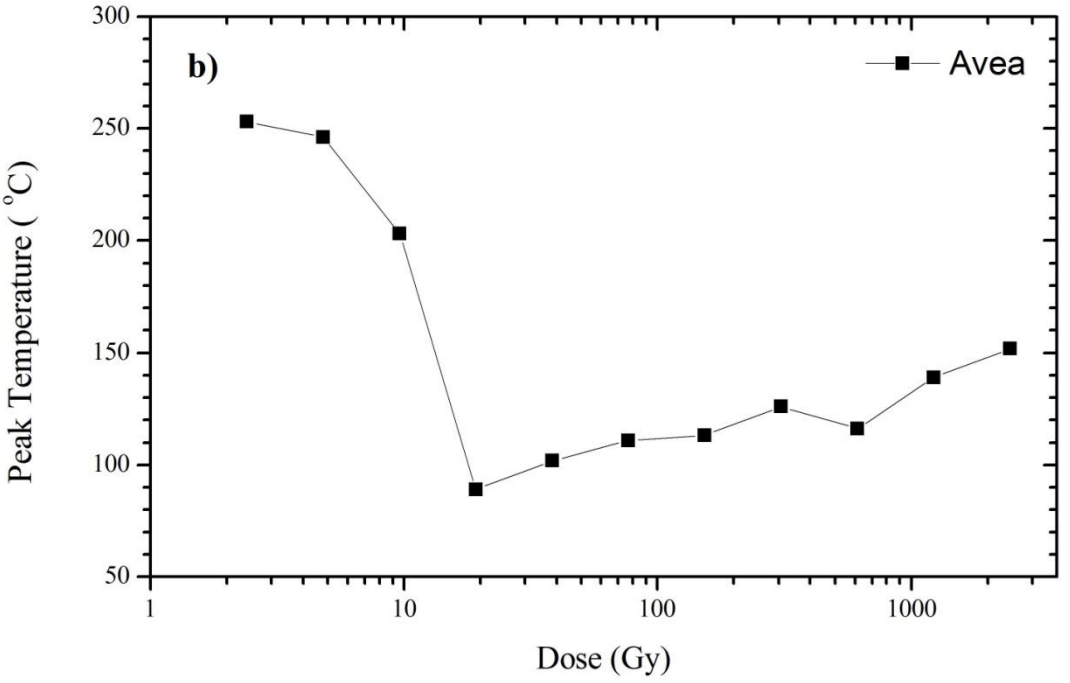

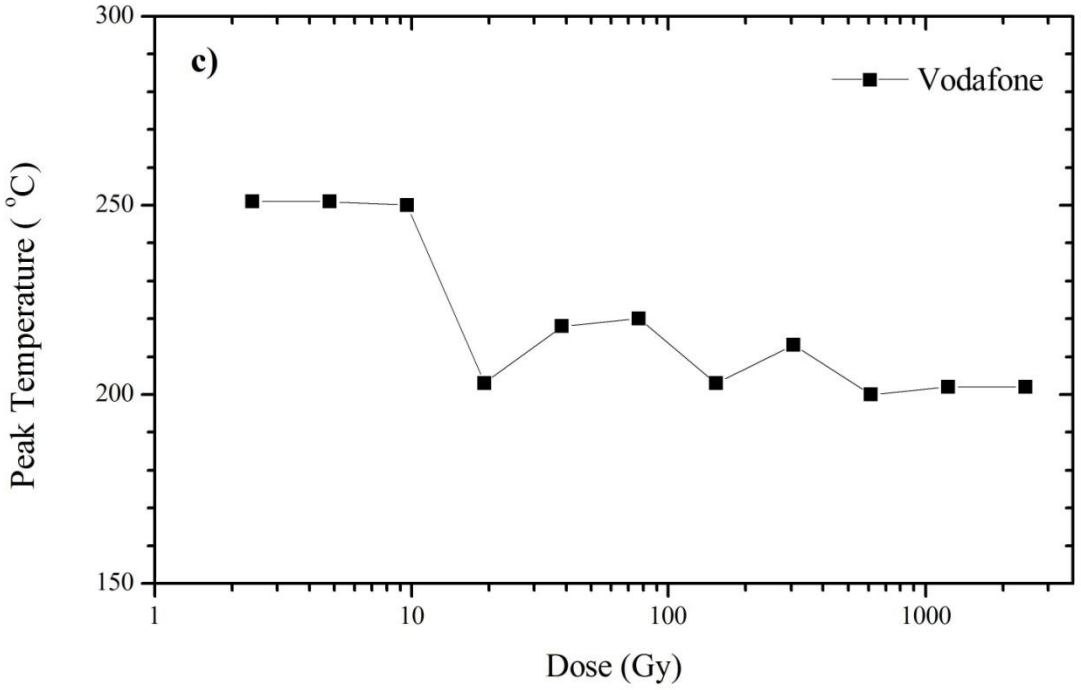

Figure 4.2 Variations of the peak temperature for different doses for the (a) Turkcell sample, (b) Avea sample, (c) Vodafone sample.

4.1.3 Variation of Maximum Thermoluminescence Intensity

In this part of the study, the effects of the different doses on the maximum thermoluminescence intensity were investigated.

Figure 4.3 shows the variations of the maximum thermoluminescence intensity as a function of doses for the (a) Turkcell sample, (b) Avea sample, and (c) Vodafone sample. In Figure 4.3 (a) if the dose increases, the maximum thermoluminescence intensity increases. In the low dose region, from to , the graph nearly acts as a supralinear. From to the graph line becomes linear. After dose, graph becomes sublinear. In this part of experiment the graph linearly increases so Turkcell sample has an acceptable variation. In Figure 4.3 (b) the graph is not linear. But generally, if the dose increases, thermoluminescence intensity also increases. In Figure 4.3 (c) shows us that the graph is not linear, and shows little variation. The expectation for dose versus thermoluminescence intensity graph is linearly increase. The Vodafone SIM card chip's thermoluminescence intensity initially decreases as the dose increases, remains constant through the middle doses, then fluctuates randomly at the higher doses.

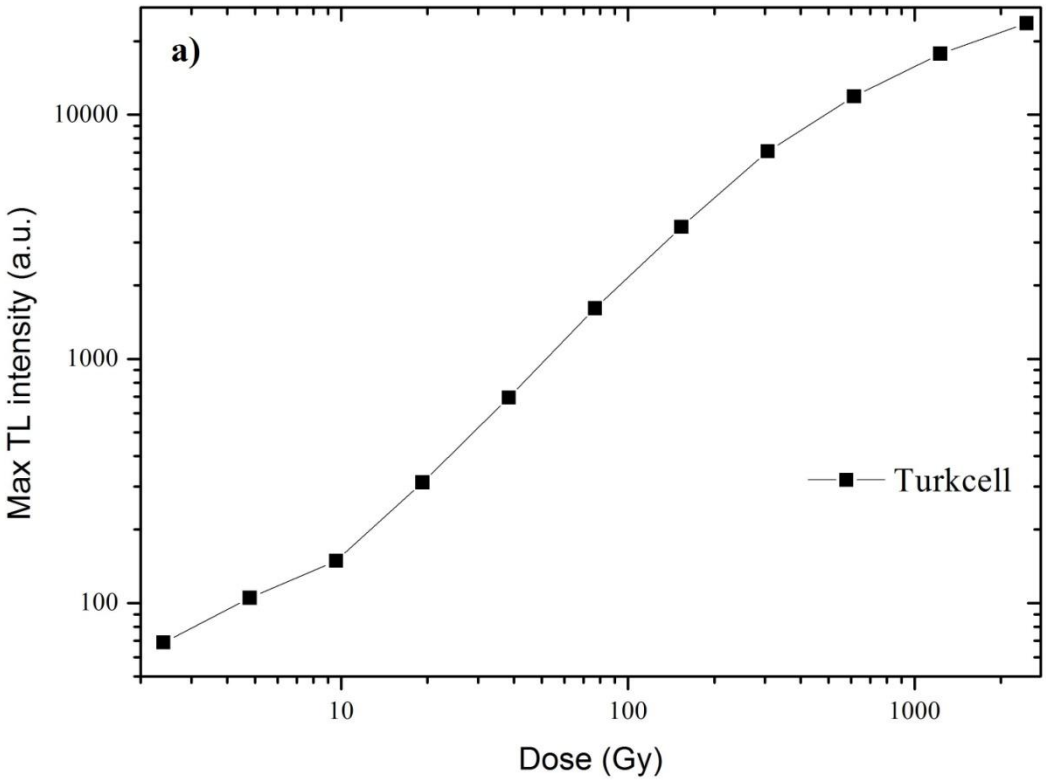
a)
Max TL intensity (a.u.)
10000
1000
100
10
100
1000
Dose (Gy)
Turkcell

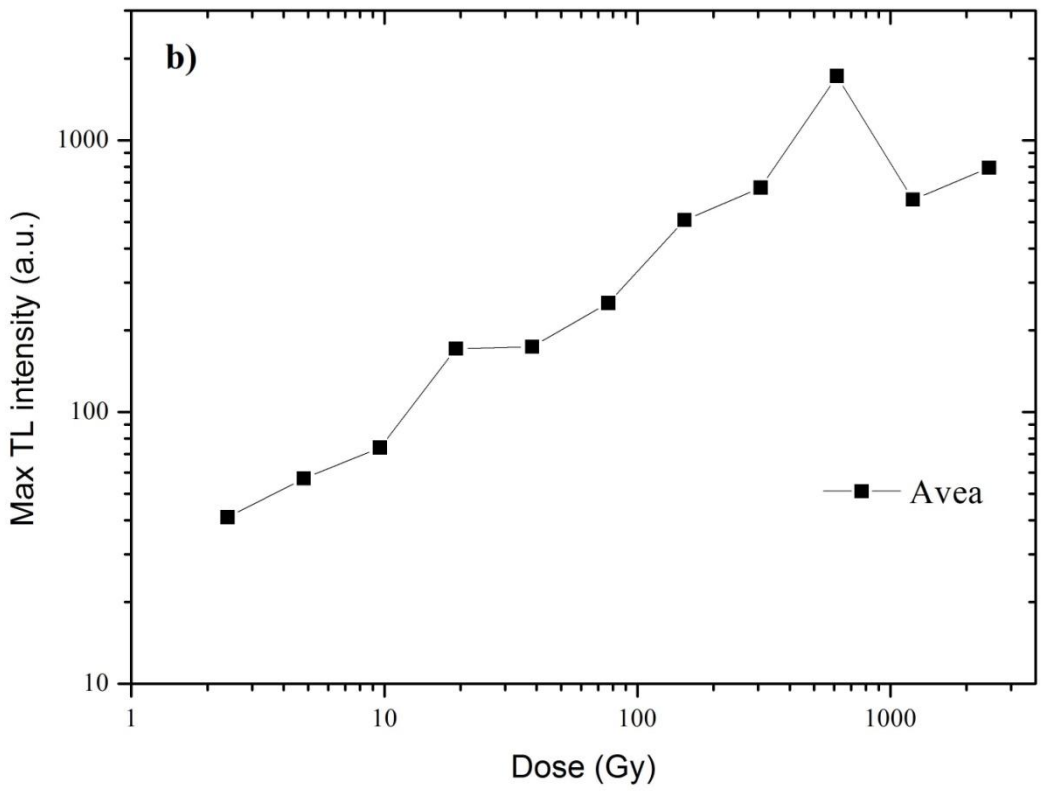
b)
Max TL intensity (a.u.)
1000
100
10
1
10
100
1000
Dose (Gy)
Avea

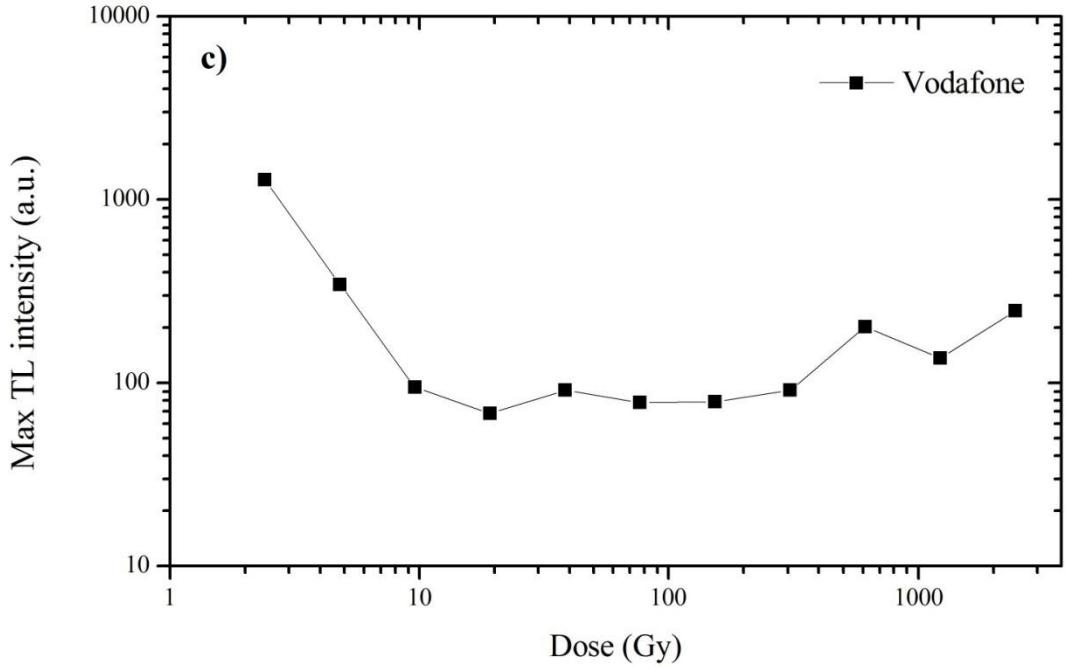

Figure 4.3 Variations of the maximum thermoluminescence intensity for different doses for the (a) Turkcell sample, (b) Avea sample, (c) Vodafone sample.

4.1.4 Variation of Area Under Curve

In this part of the experiment, the effects of the different doses on the peak area were examined.

Figure 4.4 shows the variation of area under curve as a function of doses for the (a) Turkcell sample, (b) Avea sample, and (c) Vodafone sample. In Figure 4.4 (a), in the low dose region, from to , peak area increases with increasing dose and acts as a supralinear. From to the graph line becomes linear and peak area increases with increasing dose. For high dose region, from , the graph line becomes sublinear. The expectation for dose versus peak area graph is linearly increase. And the graph generally increases linearly so Turkcell sample has acceptable results for this study. In Figure 4.4 (b), Avea sample's dose versus peak area graph is nearly linear. First the graph line increases slowly with increasing dose and acts as supralinear but after the graph line becomes linear. After the graph line becomes supralinear again. In Figure 4.4 (c), Vodafone dose versus peak area is not linear. From beginning to peak area decreases sharply with increasing dose. From to it remains constant. After there are

fluctuations. It is generally decreasing, with increasing dose. This result also does not meet our expectations for this study.

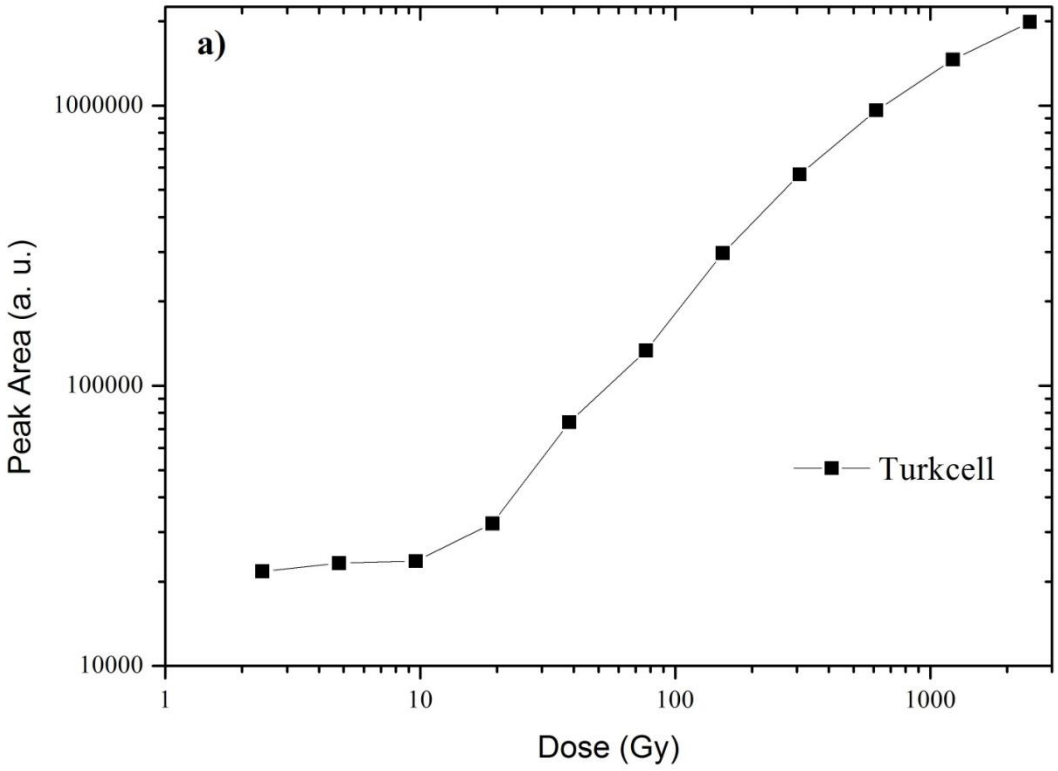

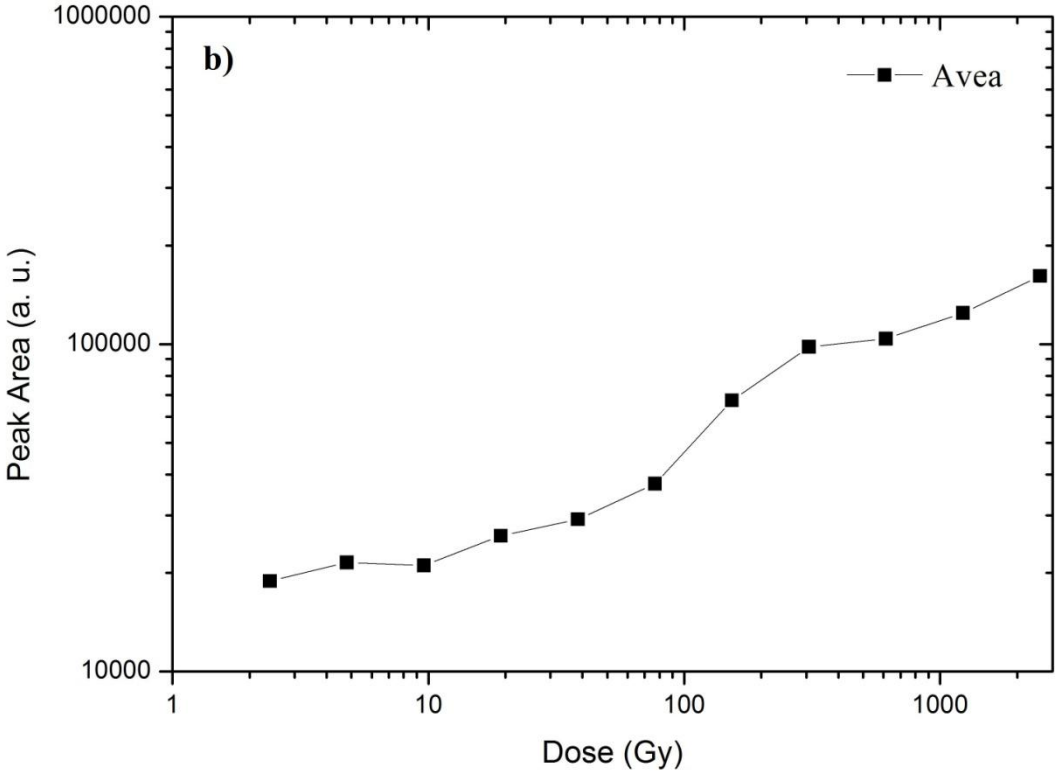

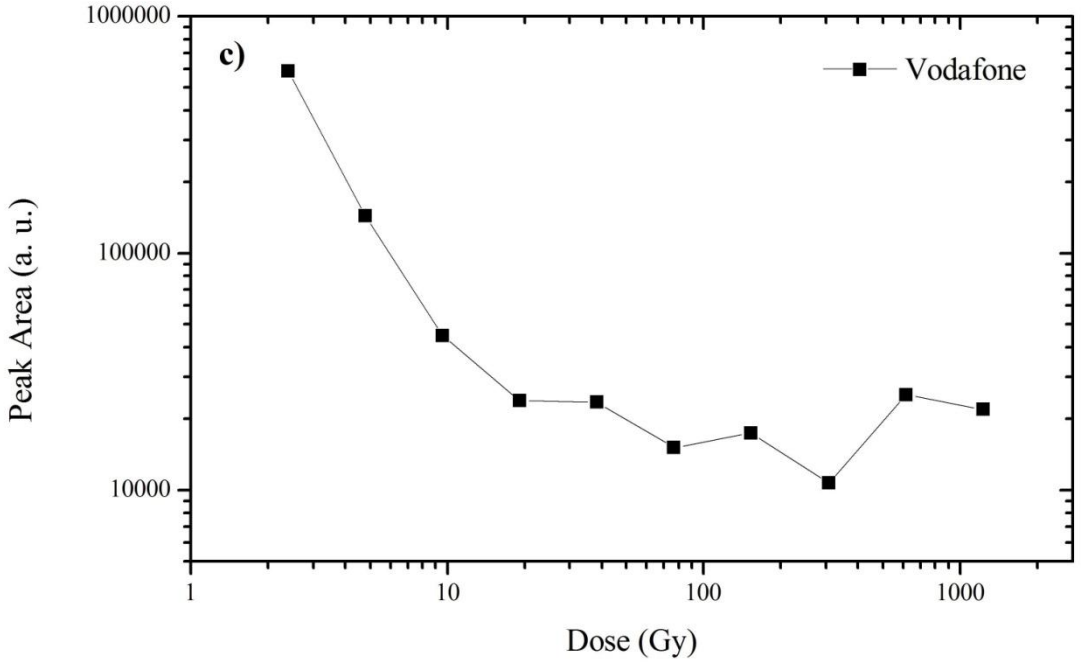

Figure 4.4 Area under curve for different doses for the (a) Turkcell sample, (b) Avea sample, (c) Vodafone sample.

4.2 Heating Rate Effect

The glow curves of samples were examined by using different heating rates during read out in this part of the experiment.

4.2.1 Variation of Glow Curve

Figure 4.5 shows variation of glow curve as a function of heating rate for the (a) Turkcell sample, (b) Avea sample, and (c) Vodafone sample. In Figure 4.5 (a), the shape of glow curves do not change by using different doses. There are no extra peaks and peaks decrease in same proportion. In Figure 4.5 (b), the shape of glow curves change by using different doses. The obtained glow curve is not good enough to make comments for Avea sample. In Figure 4.5 (c), the shape of glow curves change by using different doses. The obtained glow curve is not good enough to make comments for Vodafone sample too.

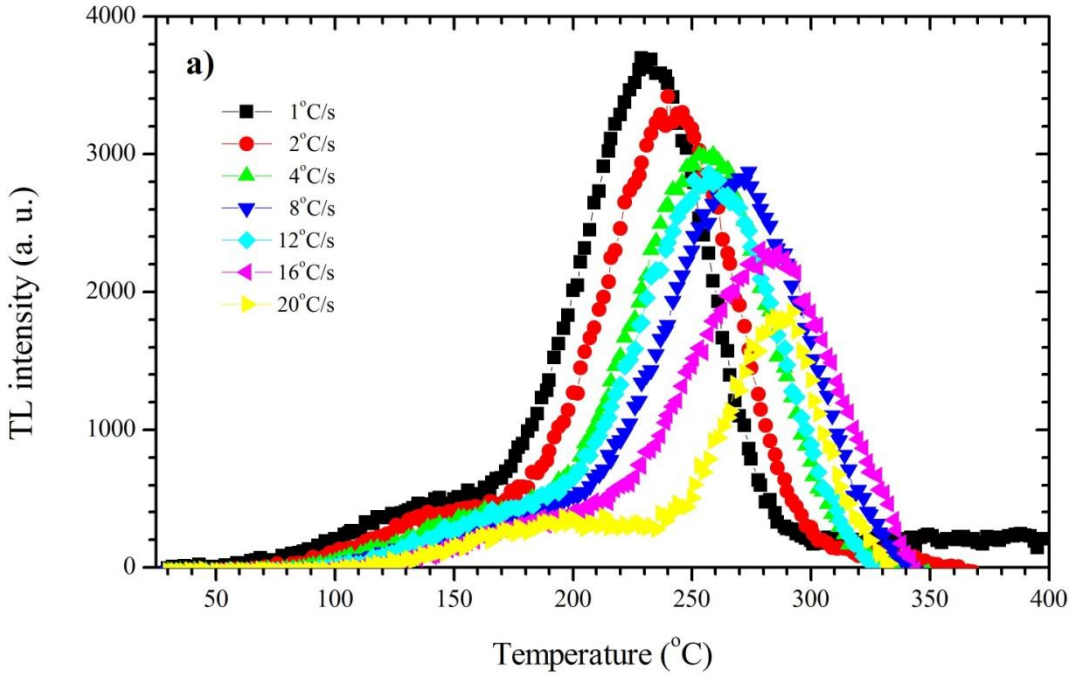
a)
1°C/s
2°C/s
4°C/s
8°C/s
12°C/s
16°C/s
20°C/s
TL intensity (a. u.)
Temperature (°C)
0
1000
2000
3000
4000
50
100
150
200
250
300
350
400

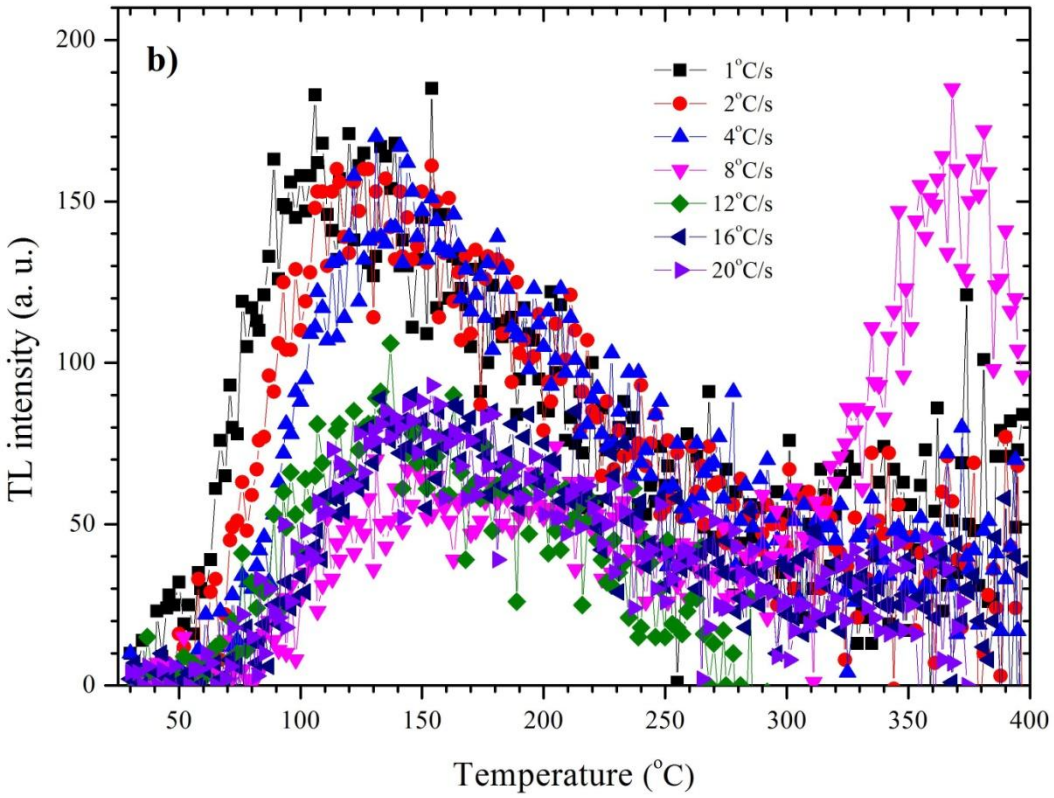
b)
1°C/s
2°C/s
4°C/s
8°C/s
12°C/s
16°C/s
20°C/s
TL intensity (a. u.)
Temperature (°C)
0
50
100
150
200
50
100
150
200
250
300
350
400

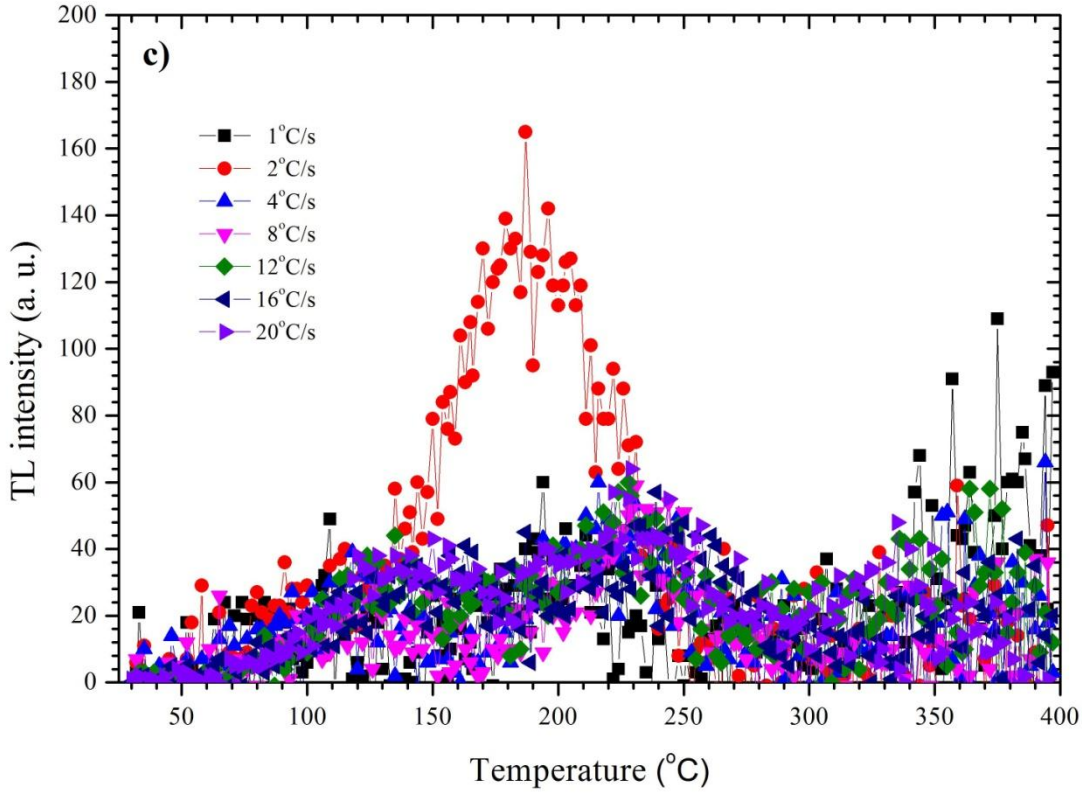

Figure 4.5 Glow curve variations for different heating rates for the (a) Turkcell sample, (b) Avea sample, (c) Vodafone sample.

4.2.2 Variation of Peak Temperature

In this part of the study, the effects of the different heating rates during read out on peak temperature were examined with heating rate of . Figure 4.6 shows the variations of the peak temperature as a function of heating rates for the (a) Turkcell sample, (b) Avea sample, and (c) Vodafone sample. In Figure 4.6 (a), if heating rates increase, peak temperature increases to the heating rate of After the heating rate of , the peak temperature decreases. When the heating rate passed the , it begins to increase again. In Figure 4.6 (b), there are fluctuations. First, the peak temperature remains constant. After the heating rate of , there are fluctuations for peak temperature. When it passed the heating rate of , the peak temperature begins to increase. Generally, the thermoluminescence glow curve of Avea sample has not good data to make comments about the peak temperature. In Figure 4.6 (c), peak temperature decreases at the beginning. Then it started to increase after the heating rate of . But this increment is not linear. Then at the end there are fluctuations for peak temperature.

Generally, the thermoluminescence glow curve of Vodafone sample has not good data to make comments about peak temperature too.

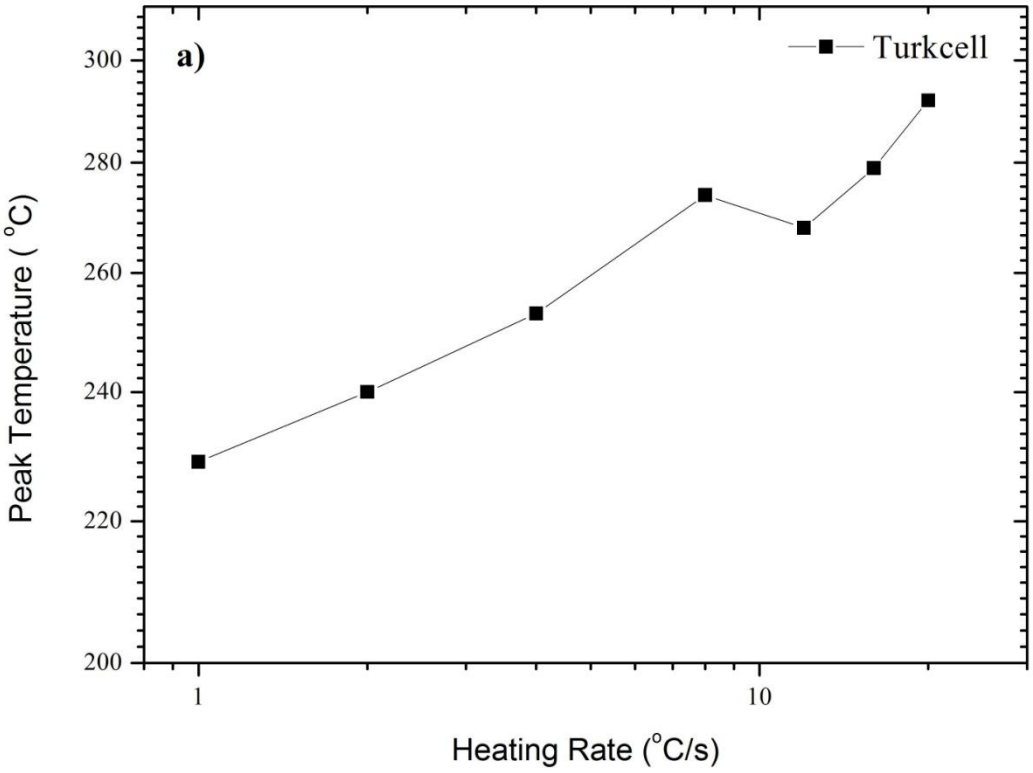

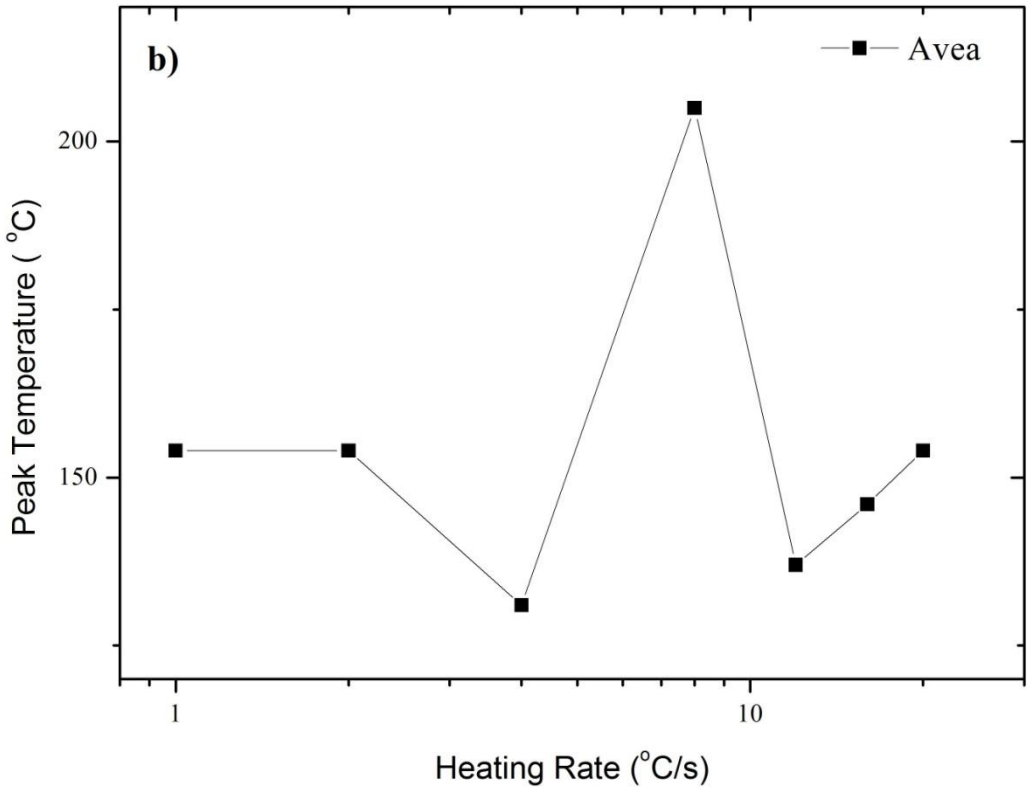

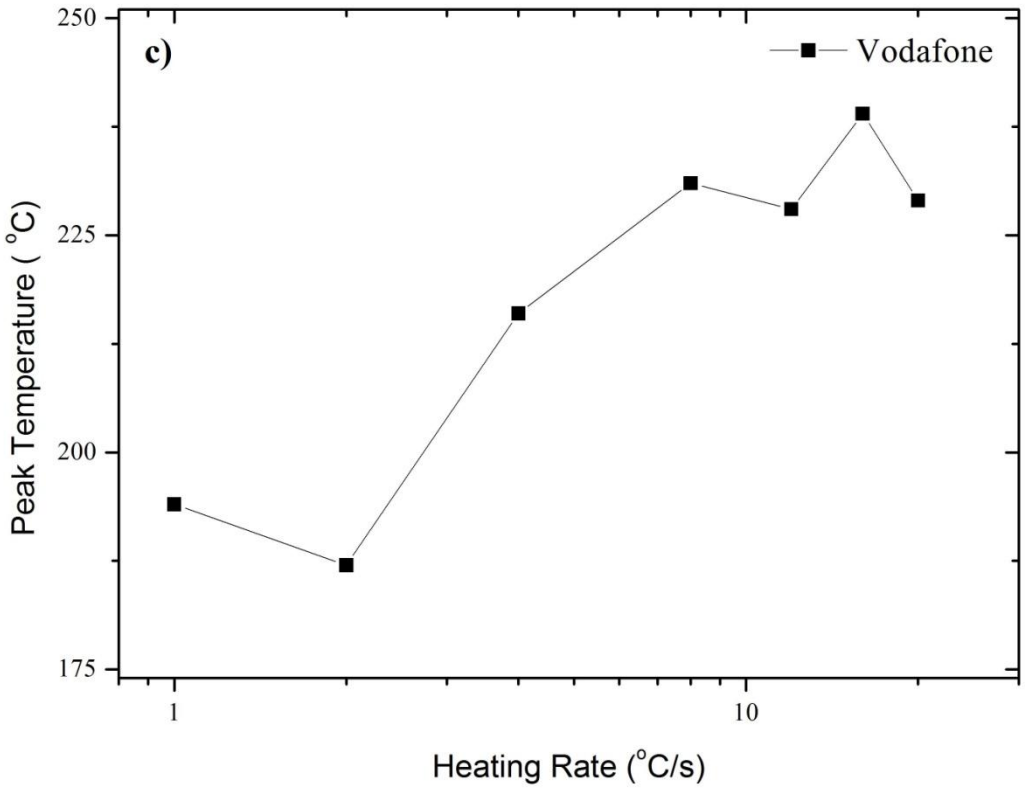

Figure 4.6 Variations of peak temperature for different heating rates for the (a) Turkcell sample, (b) Avea sample, (c) Vodafone sample.

4.2.3 Variation of Maximum Thermoluminescence Intensity

In this part of the experiment, the effects of the differents heating rates on the maximum thermoluminescence intensity were examined.

Figure 4.7 shows variation of maximum thermoluminescence intensity as a function of heating rate for the (a) Turkcell sample, (b) Avea sample, and (c) Vodafone sample. In Figure 4.7 (a), if the heating rate increases, the maximum thermoluminescence intensity decreases. After the heating rate of , the maximum thermoluminescence intensity decreases sharply. There was a photonic error in the TLD reader during the reading process after the heating rate of . In Figure 4.7 (b), the maximum thermoluminescence intensity remains constant from the heating rate to 4 . After the heating rate of 4 there are fluctuations. The maximum thermoluminescence intensity only decreases for a small section of the graph. The glow curve of Avea sample has not good data to make comments about the maximum thermoluminescence intensity. In Figure 4.7 (c), with the exception of a spike at the heating rate of , the maximum thermoluminescence intensity

remains constant. The glow curve of Vodafone sample has not good data to make comments about maximum thermoluminescence intensity too.

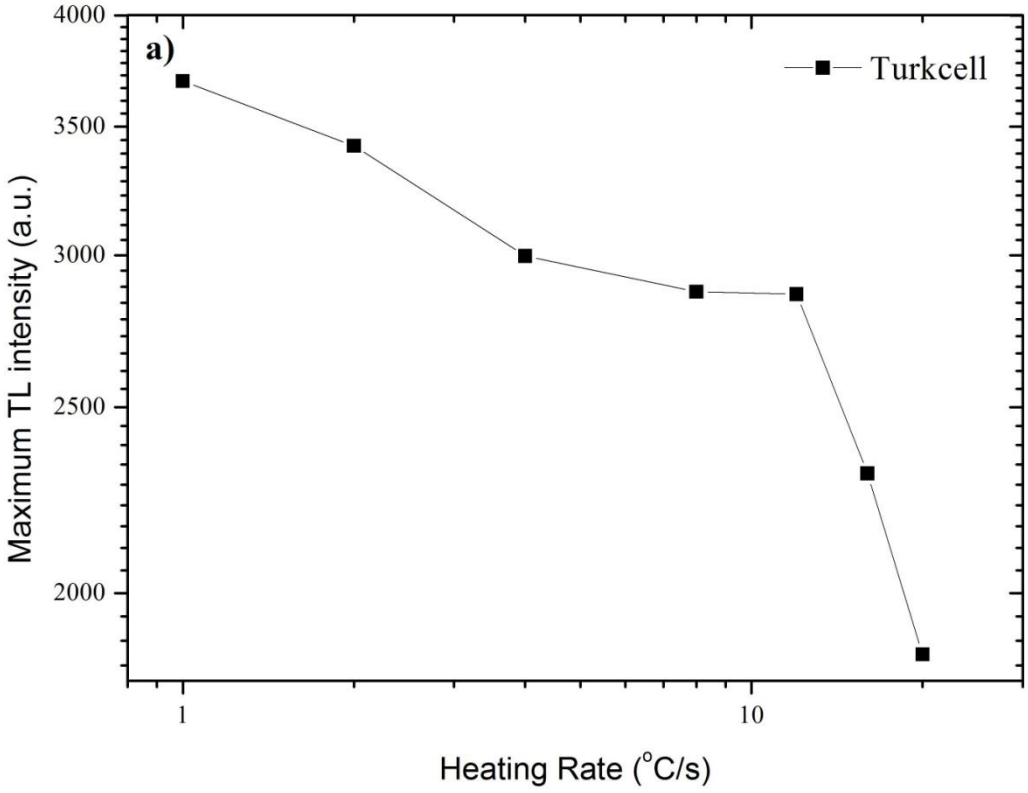

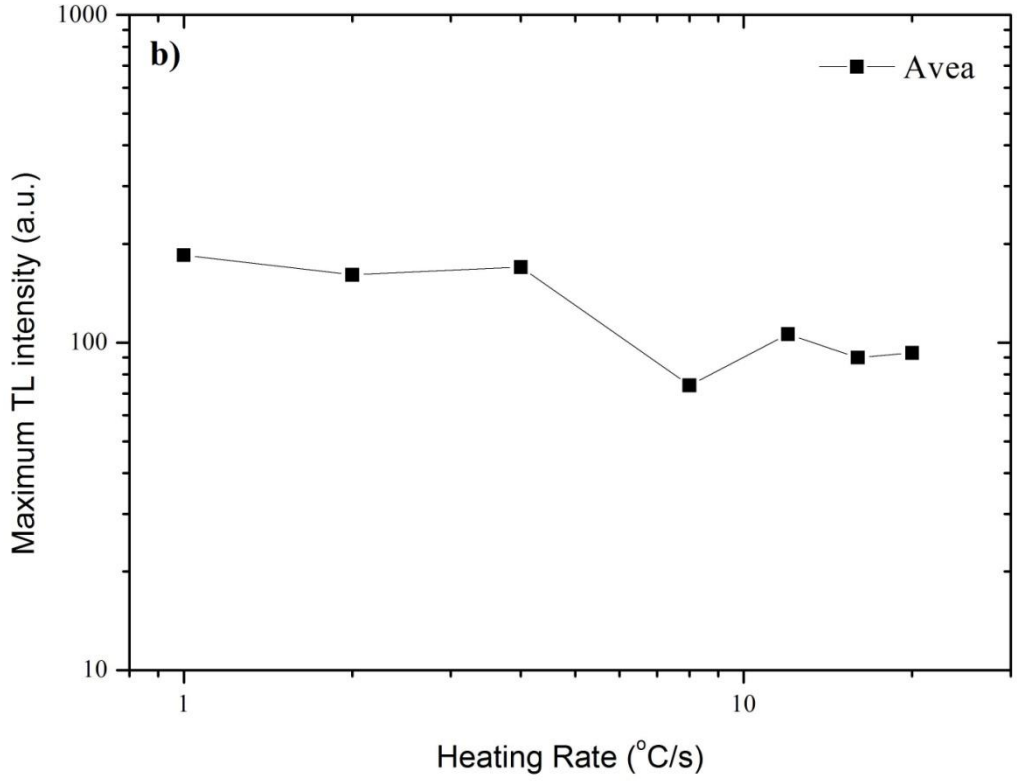

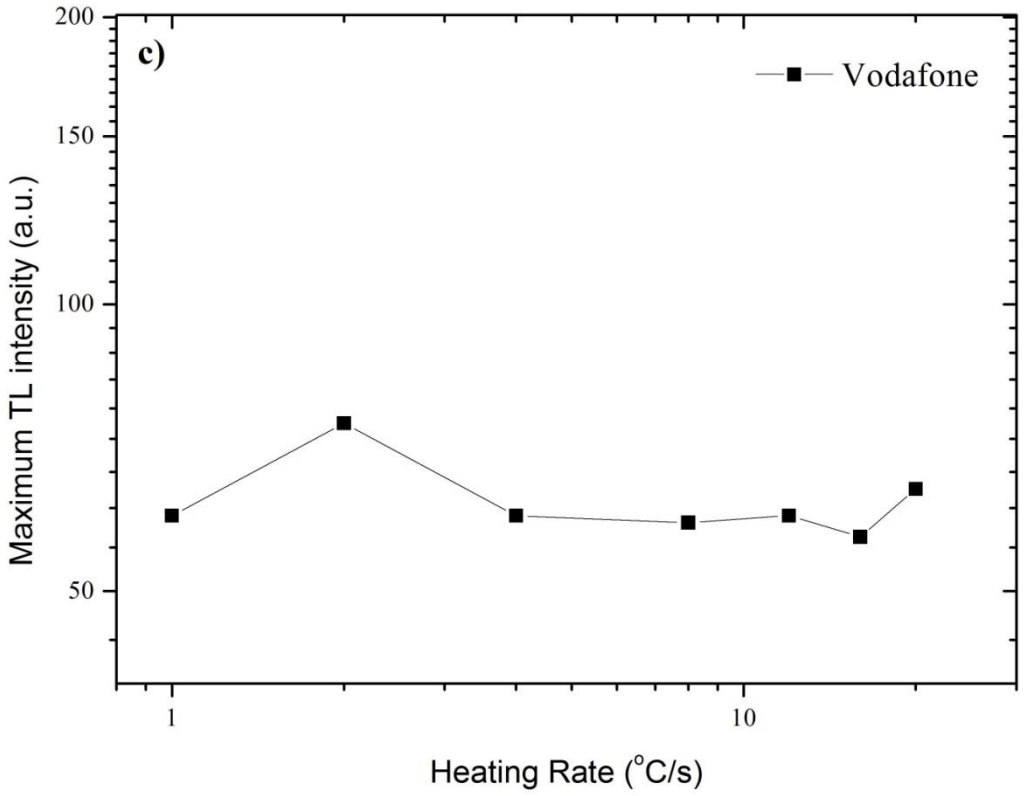

Figure 4.7 Variations of maximum thermoluminescence intensity for different heating rates for the (a) Turkcell sample, (b) Avea sample, (c) Vodafone sample.

4.2.4 Variation of Area Under Curve

In this part of the study, the effects of the different heating rates on the peak area were examined.

Figure 4.8 shows variation of area under curve as a function of the heating rate for the (a) Turkcell sample, (b) Avea sample, and (c) Vodafone sample. In Figure 4.8 (a), the peak area decreases with increasing heating rates. It is not linear but it continually decreases. After the heating rate of , the peak area decreases sharply. There was a photonic error in the TLD reader during the reading process after the heating rate of . In Figure 4.8 (b), the peak area decreases slightly with increasing heating rates. There is a sharp decrement and increment between the heating rate of and . There was a photonic error in the TLD reader during the reading process with the heating rate of . In Figure 4.8 (c), there are many fluctuations with increasing heating rates.

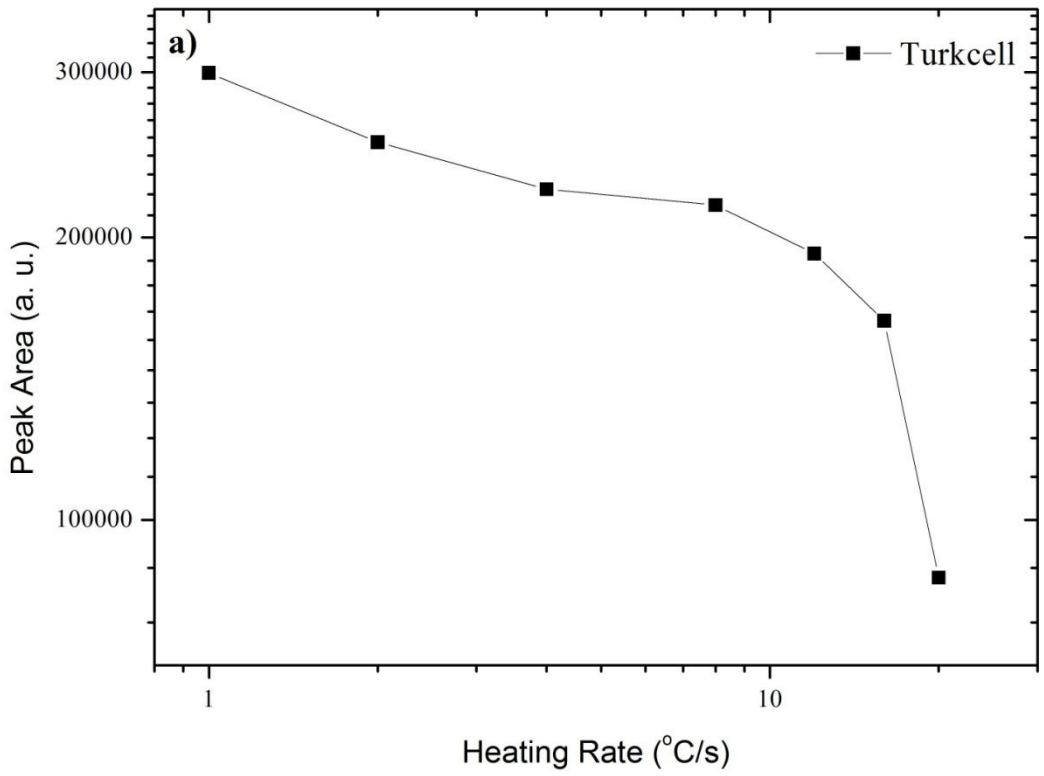
a)
Turkcell
300000
200000
100000
Peak Area (a. u.)
1
10
Heating Rate (°C/s)

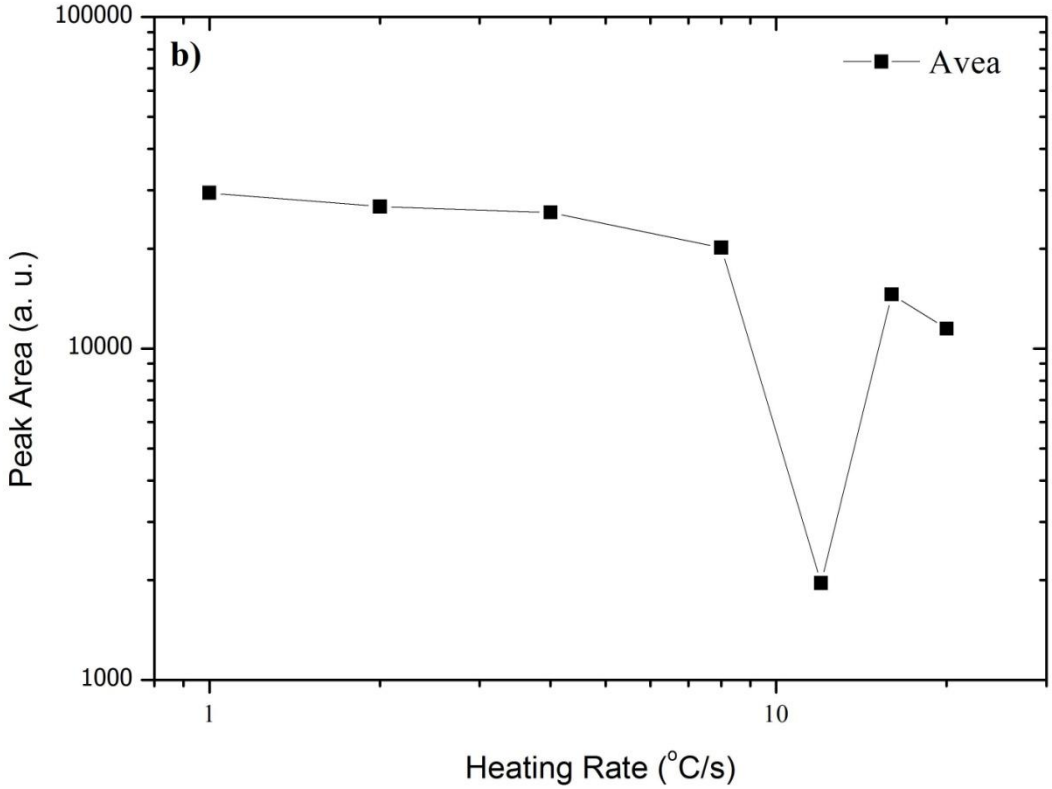
b)
Avea
100000
10000
1000
Peak Area (a. u.)
1
10
Heating Rate (°C/s)

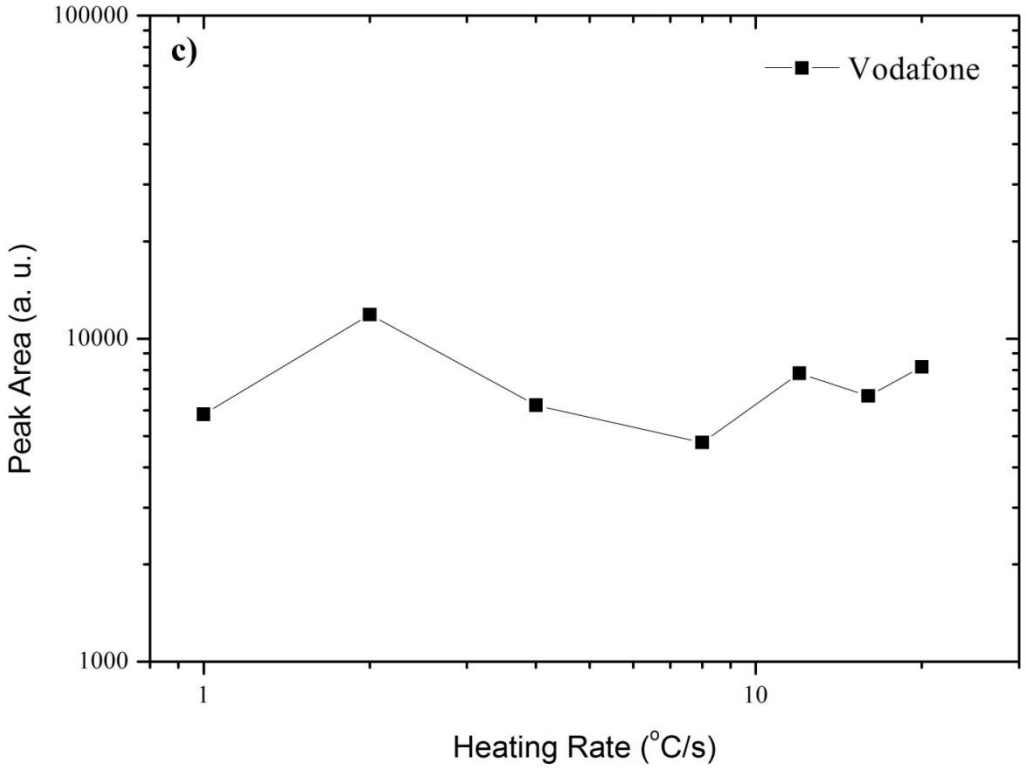

Figure 4.8 Area under curve for different heating rates for the (a) Turkcell sample, (b) Avea sample, (c) Vodafone sample.

4.3 Cycle of Measurements

The reproducibilities of samples were investigated with repeated experiments in this part.

4.3.1 Variation of Glow Curve

Figure 4.9 shows variations of the glow curve for the (a) Turkcell sample, (b) Avea sample, and (c) Vodafone sample. In Figure 4.9 (a), the thermoluminescence intensities have approximately same results for eight experiments. In Figure 4.9 (b), each experiment gives different results. There is no repeatability. In Figure 4.9 (c), some experiments have the same results. But some of them have different results so there is no proven repeatability.

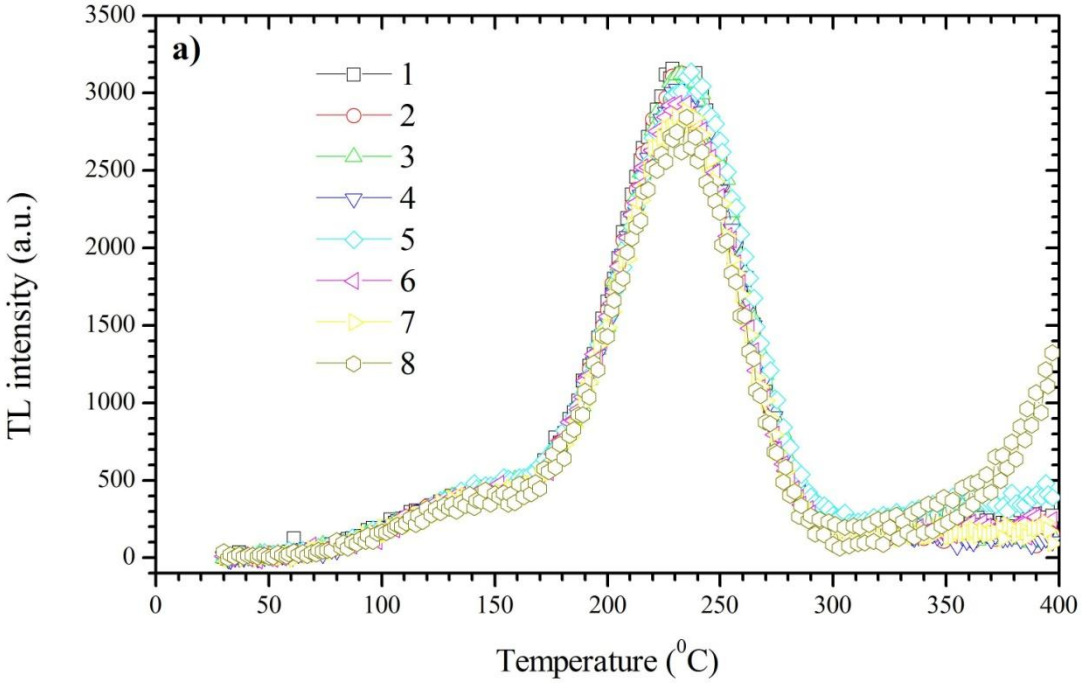
a)
1
2
3
4
5
6
7
8
TL intensity (a.u.)
Temperature (^{0}C)
0
500
1000
1500
2000
2500
3000
3500
0
50
100
150
200
250
300
350
400

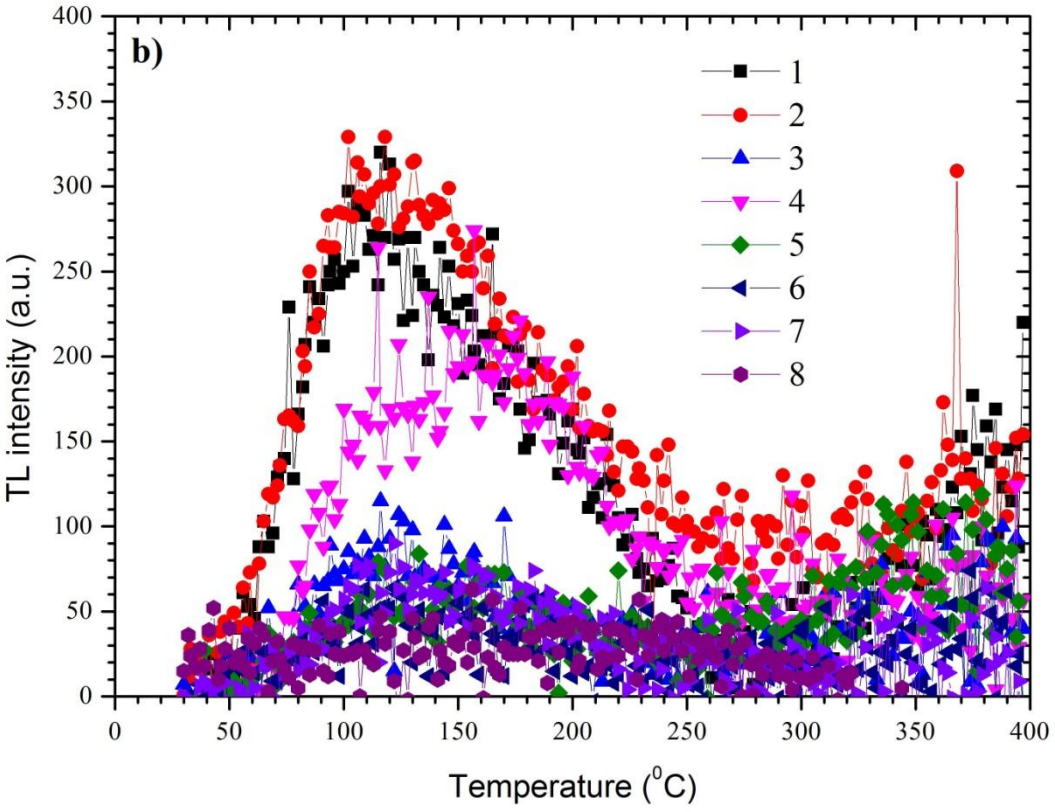
b)
1
2
3
4
5
6
7
8
TL intensity (a.u.)
Temperature (^{0}C)
0
50
100
150
200
250
300
350
400
0
50
100
150
200
250
300
350
400

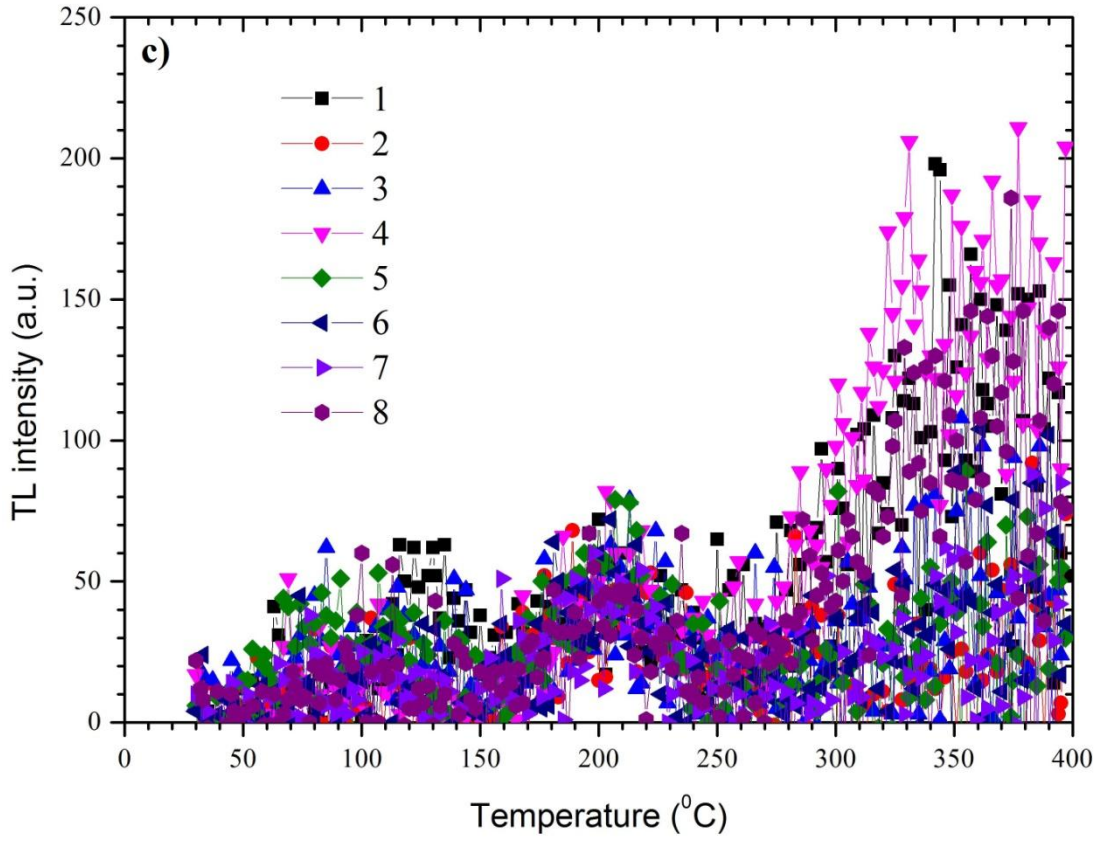

Figure 4.9 Glow curve variations for the (a) Turkcell sample, (b) Avea sample, (c)Vodafone sample.

4.3.2 Normalized Maximum Thermoluminescence Intensity

The maximum thermoluminescence intensity of each sample was examined and normalization was made for a better comparison.

Figure 4.10 shows variations of normalized maximum thermoluminescence intensity for the (a) Turkcell sample, (b) Avea sample, and (c) Vodafone sample. In Figure 4.10 (a), each experiment has approximately the same result and they were close enough to 1. The repeatability is valid for the maximum thermoluminescence intensity of the Turkcell sample. In Figure 4.10 (b), there are fluctuations and results are different from each other. The repeatability is not valid for maximum thermoluminescence intensity of the Avea sample. In Figure 4.10 (c), there are some fluctuations but variations are not large. The repeatability may be valid for maximum thermoluminescence intensity of the Vodafone sample.

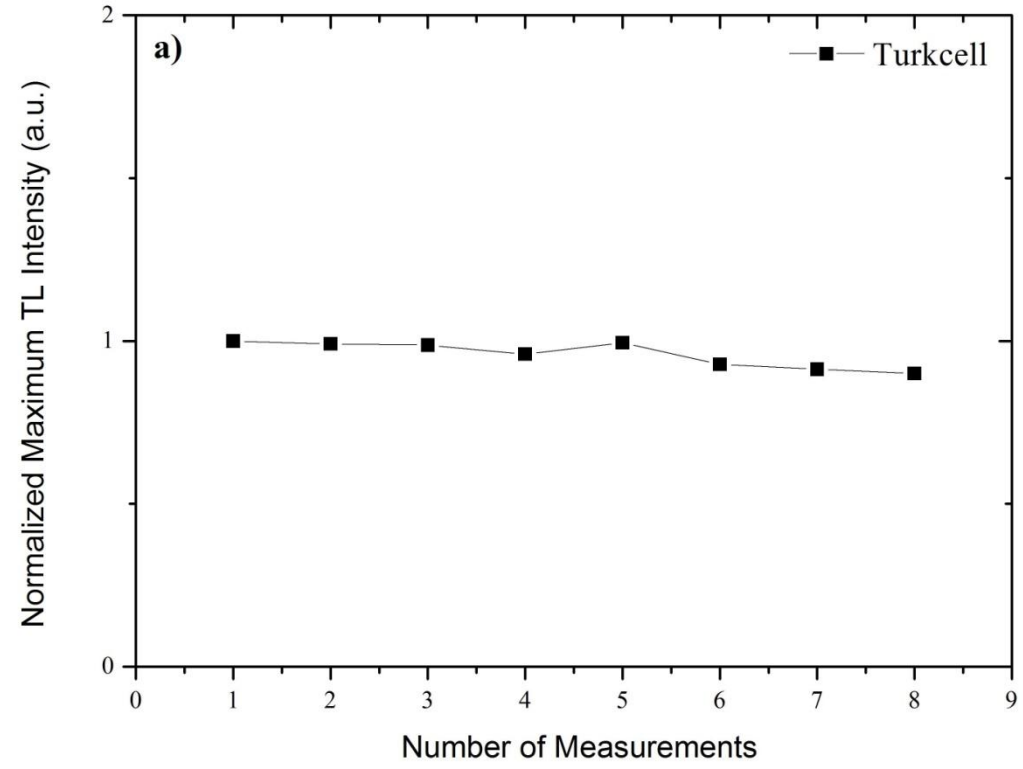
a)
Turkcell
Normalized Maximum TL Intensity (a.u.)
Number of Measurements
0
1
2
0
1
2
3
4
5
6
7
8
9

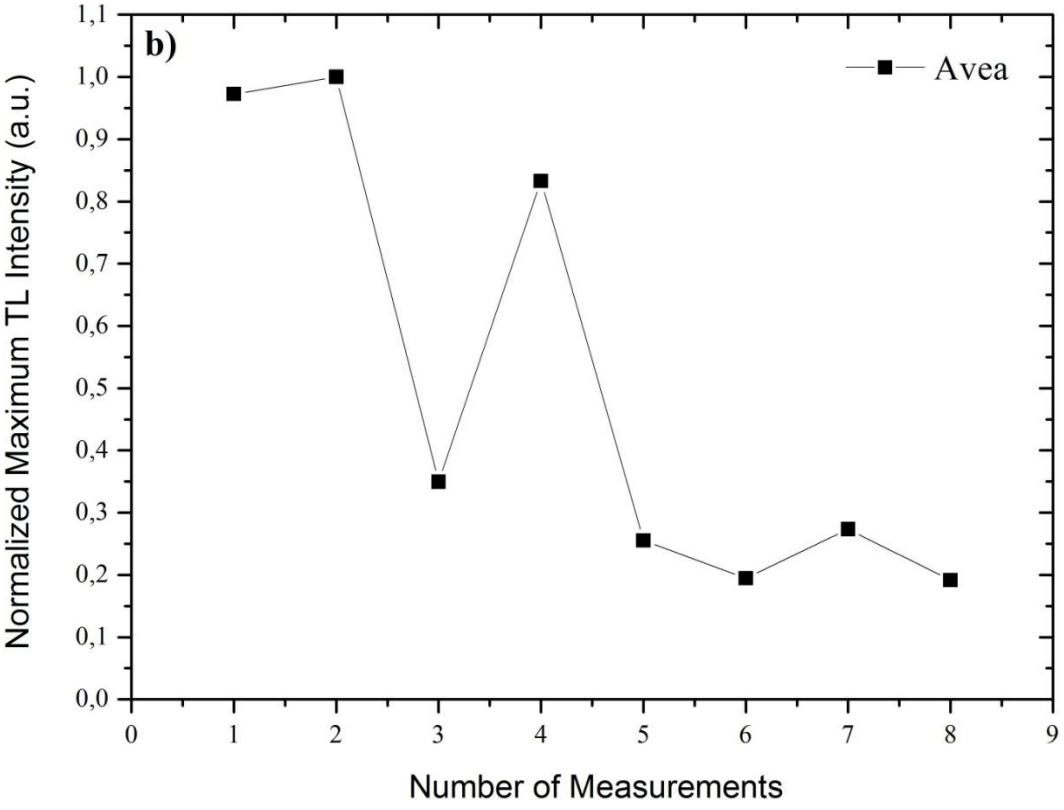
b)
Avea
Normalized Maximum TL Intensity (a.u.)
Number of Measurements
0,0
0,1
0,2
0,3
0,4
0,5
0,6
0,7
0,8
0,9
1,0
1,1
0
1
2
3
4
5
6
7
8
9

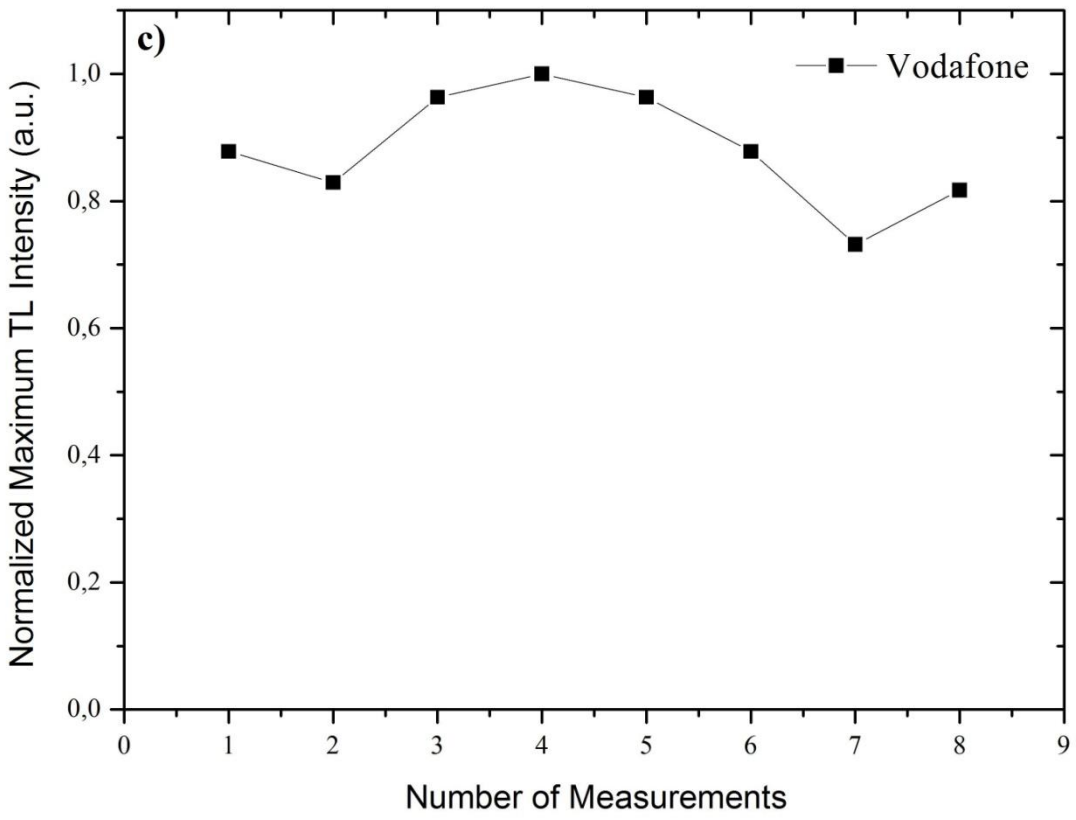

Figure 4.10 Normalized thermoluminescence intensity for the (a) Turkcell sample, (b) Avea sample, (c) Vodafone sample.

From experimental data of normalized maximum thermoluminescence intensity, mean (average), standard deviation, variance (standard deviation), population standard deviation, and variance (population standard deviation) were calculated. For Turkcell sample:

Table 4.1 Mean, standard deviation, and variance of Turkcell sample for normalized maximum thermoluminescence intensity

Mean (Average)	0.95943
Standard deviation	0.04019
Variance(Standard deviation)	0.00162
Population Standard deviation	0.03759
Variance(Population Standard deviation)	0.00141

For Avea sample:

Table 4.2 Mean, standard deviation, and variance of Avea sample for normalized maximum thermoluminescence intensity

Mean (Average)	0.5087
Standard deviation	0.35974
Variance(Standard deviation)	0.12941
Population Standard deviation	0.33651
Variance(Population Standard deviation)	0.11324

For Vodafone sample:

Table 4.3 Mean, standard deviation, and variance of Vodafone sample for normalized maximum thermoluminescence intensity

Mean (Average)	0.88259
Standard deviation	0.09009
Variance(Standard deviation)	0.00812
Population Standard deviation	0.08427
Variance(Population Standard deviation)	0.0071

4.3.3 Normalized Area Under Curve

The area under curve of each sample was investigated and the normalization was made for a better comparison.

Figure 4.11 shows variations of normalized area under curve for the (a) Turkcell sample, (b) Avea sample, and (c) Vodafone sample. In Figure 4.11 (a), each experiment for area under curve has approximately same result and they close enough to 1. The repeatability is valid for area under curve of the Turkcell sample. In Figure 4.11 (b), there are fluctuations and results are different from each other. The repeatability is not valid for area under curve of the Avea sample. In Figure 4.11 (c), there are fluctuations and results are different from each other. The repeatability is not valid for area under curve of the Vodafone sample.

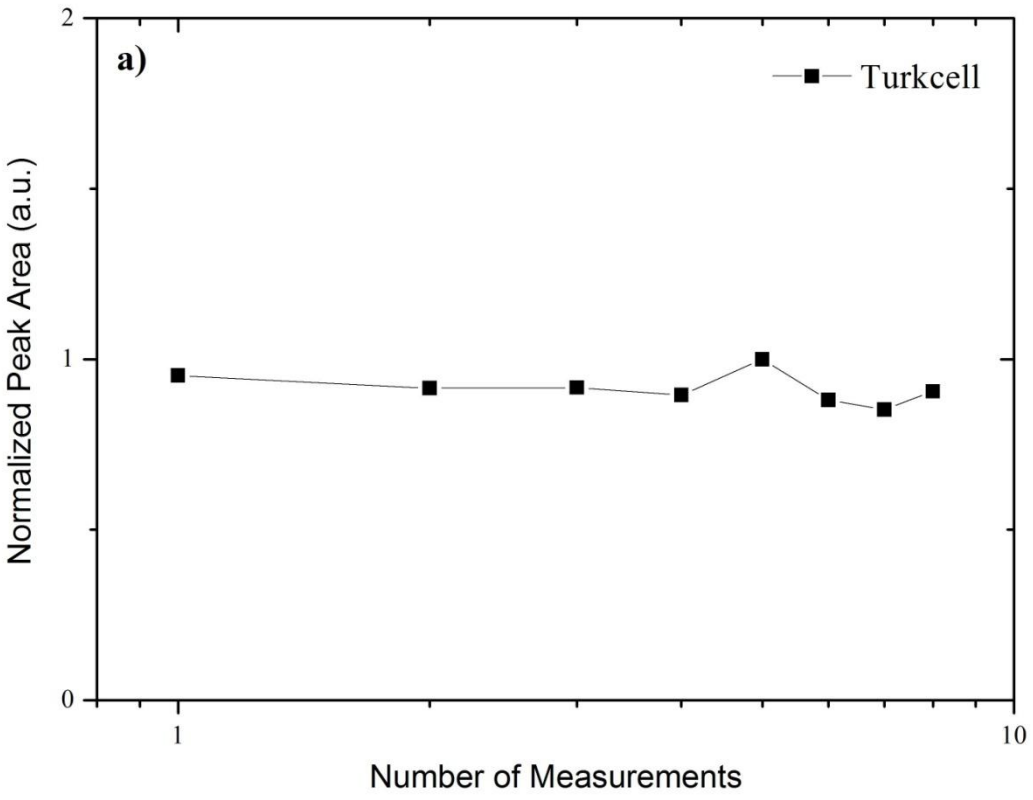
a)
Turkcell
Normalized Peak Area (a.u.)
2
1
0
1
10
Number of Measurements

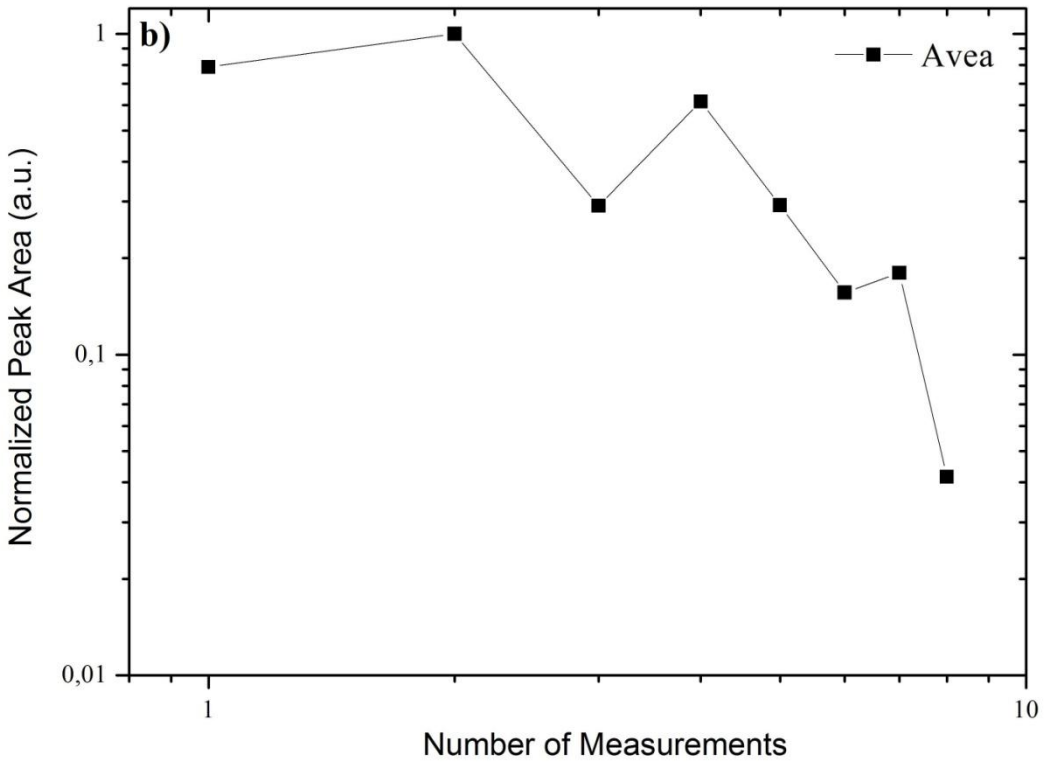
b)
Avea
Normalized Peak Area (a.u.)
1
0,1
0,01
1
10
Number of Measurements

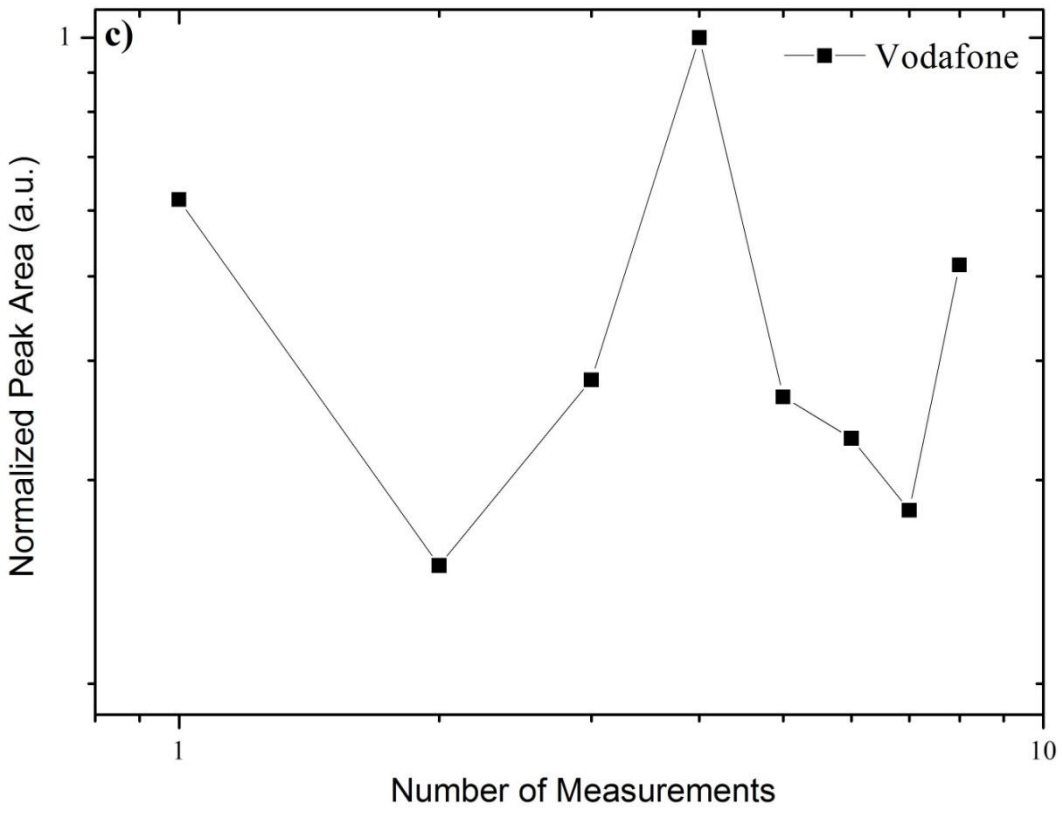

Figure 4.11 Normalized area under curve for the (a) Turkcell sample, (b) Avea sample, (c) Vodafone sample.

From experimental data of normalized area under curve, mean (average), standard deviation, variance (standard deviation), population standard deviation, and variance (population standard deviation) were calculated too. For Turkcell sample:

Table 4.4 Mean, standard deviation, and variance of Turkcell sample for normalized area under curve

Mean (Average)	0.91488
Standard deviation	0.045
Variance(Standard deviation)	0.00202
Population Standard deviation	0.04209
Variance(Population Standard deviation)	0.00177

For Avea sample:

Table 4.5 Mean, standard deviation, and variance of Avea sample for normalized area under curve

Mean (Average)	0.42073
Standard deviation	0.34101
Variance(Standard deviation)	0.11629
Population Standard deviation	0.31898
Variance(Population Standard deviation)	0.10175

For Vodafone sample:

Table 4.6 Mean, standard deviation, and variance of Vodafone sample for normalized area under curve

Mean (Average)	0.40846
Standard deviation	0.27479
Variance(Standard deviation)	0.07551
Population Standard deviation	0.25704
Variance(Population Standard deviation)	0.06607

4.4 Fading Effect

The irradiated samples of Turkcell, Avea, and Vodafone SIM card chips were placed in a box in a completely dark environment to protect from light contamination and were held for different time intervals. The glow curves of samples were examined by using different waiting time in the dark environment in this part of the experiments. The aim of fading effect was how much the dose is lost after radiation and waiting process.

4.4.1 Variation of Glow Curve

Figure 4.12 shows the variation of glow curve as a function of waiting time in the dark environment for the (a) Turkcell sample, (b) Avea sample, and (c) Vodafone sample. In Figure 4.12 (a), the shape of glow curves do not change by using different

waiting time. There are no extra peaks and peaks increase in same proportion. In Figure 4.12 (b), the shape of glow curves change by using different waiting time. There are extra peaks and peaks are not increased in same proportion.

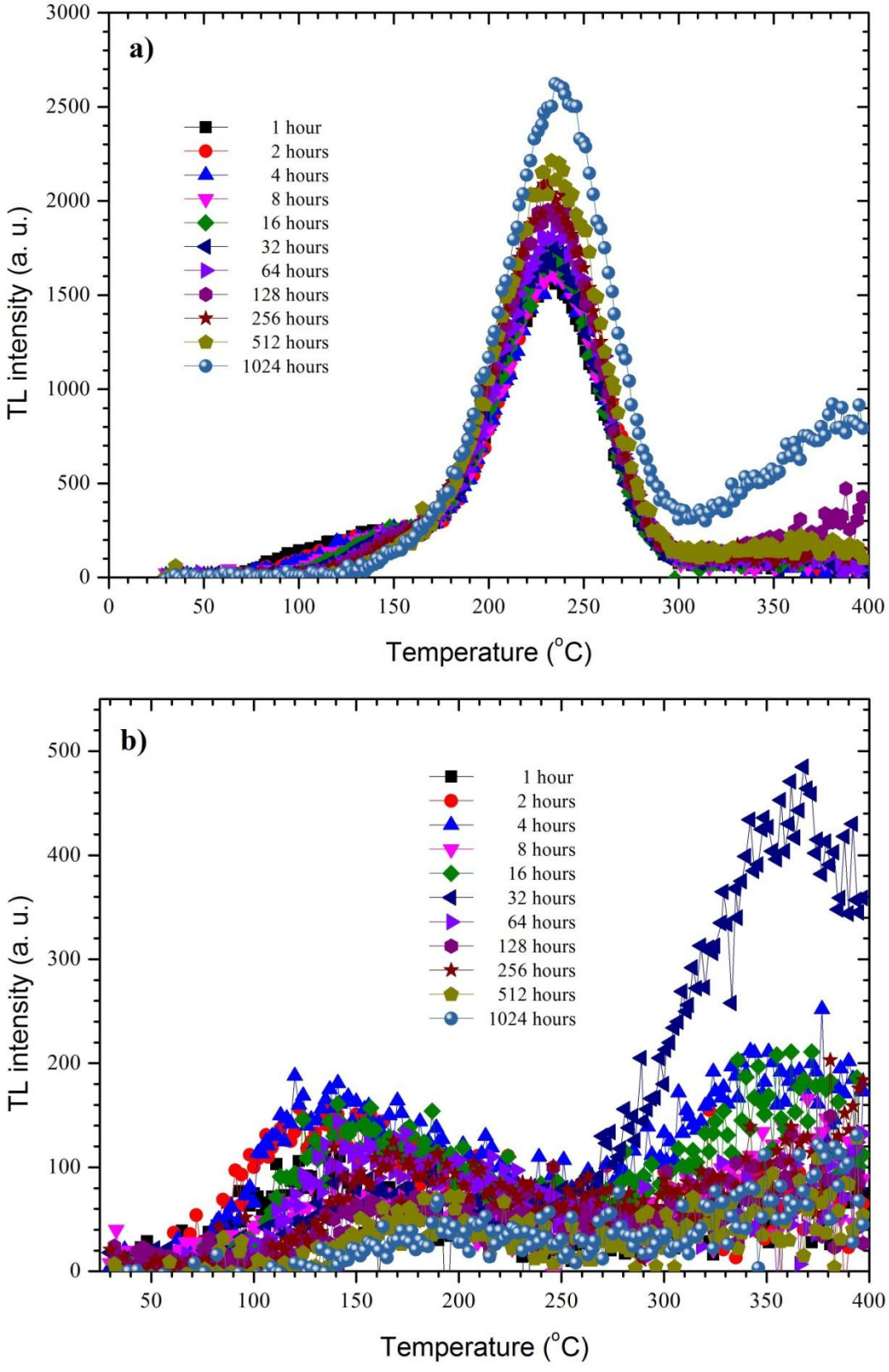

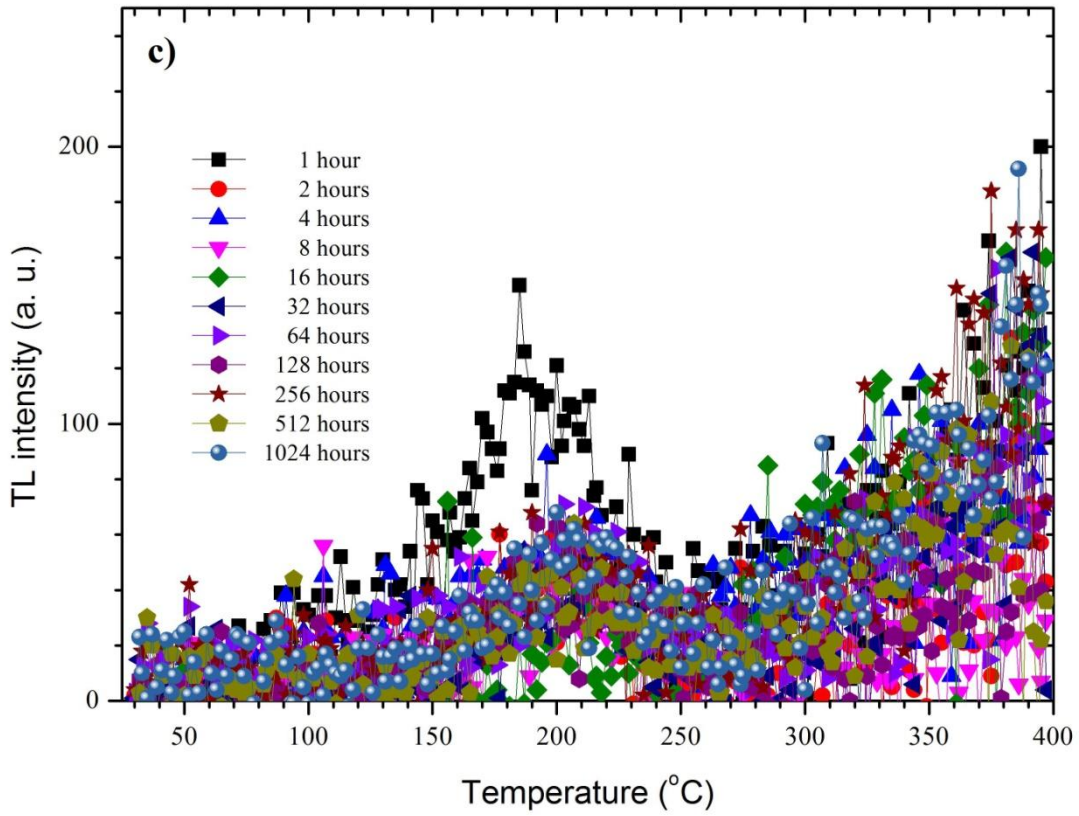

Figure 4.12 Variations of glow curve for different waiting time in the dark environment for the (a) Turkcell sample, (b) Avea sample, (c) Vodafone sample.

So this sample is not suitable for precision radiation intensity measurements based on the glow curve. In Figure 4.12 (c), the thermoluminescence intensities are not increasing properly with increasing waiting time. On the other hand there are not any peaks in the glow curve for taking information about sample. This sample is also not suitable for precision radiation intensity measurements based on the glow curve.

4.4.2 Variation of Peak Temperature

In this part of the experiment, the effects of the different waiting time in the dark on the peak temperatures of thermoluminescence intensity were examined.

Figure 4.13 shows the variations of peak temperature as a function of the waiting time for the (a) Turkcell sample, (b) Avea sample, and (c) Vodafone sample. In Figure 4.13 (a), if the waiting time increases, the peak temperature increases or decreases randomly. Before waiting time there are fluctuations. Between and the peak temperature remains constant. After the peak temperature begins to decrease. And finally after it begins to

increase as a linear. In Figure 4.13 (b), the peak temperature increases or decreases randomly. And there are lots of fluctuations. But the data of

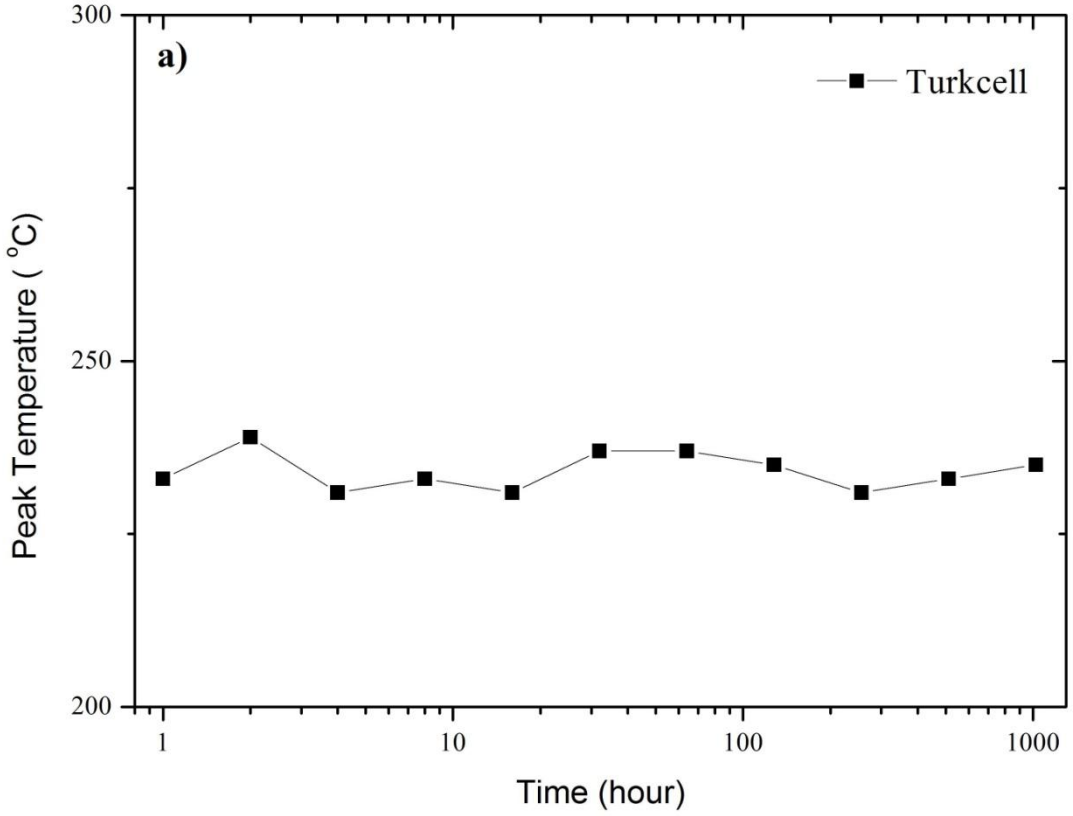

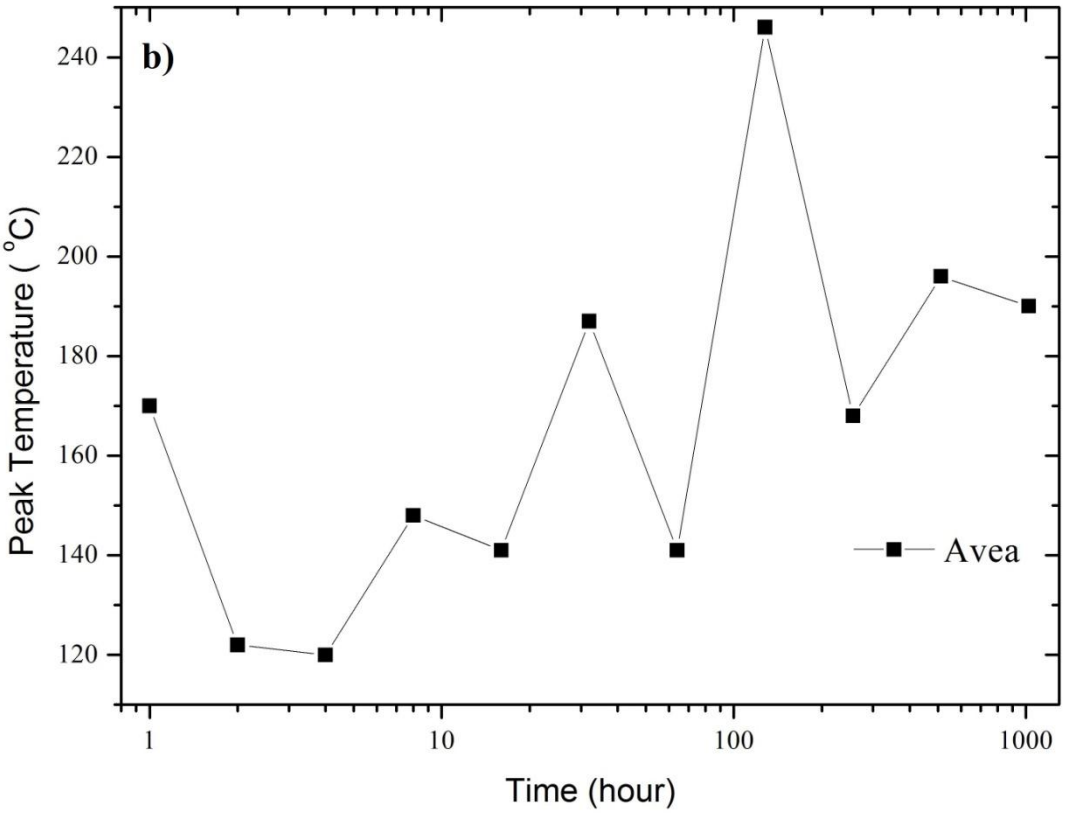

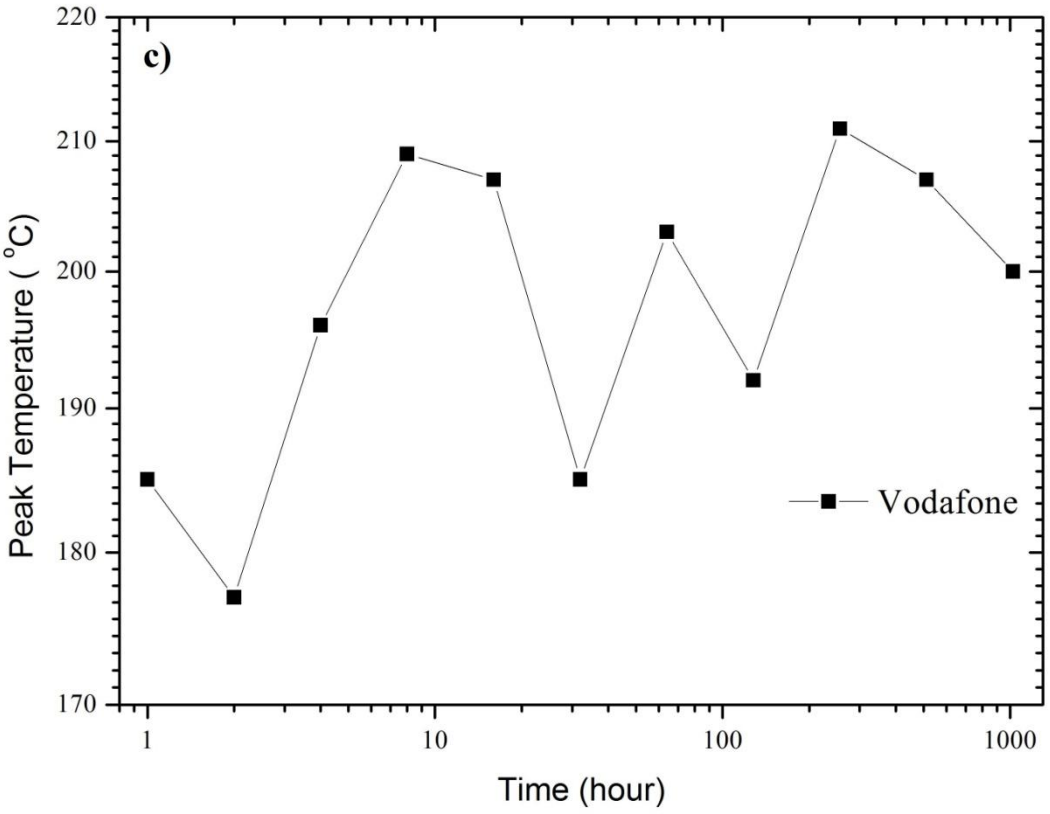

Figure 4.13 Variations of peak temperature for different waiting time in the dark for the (a) Turkcell sample, (b) Avea sample, (c) Vodafone sample.

glow curve are not good enough to make comments for Avea sample. In Figure 4.13 (c), the peak temperature decreases with increasing the waiting time. Between and the peak temperature increases with increasing the waiting time. After the peak temperature begins to decrease. There is a sharply decrease at . Between and the peak temperature increases and decreases randomly. After the peak temperature decreases with increasing the waiting time. But the obtained glow curve is not good enough to make comments for Vodafone sample too.

4.4.3 Variation of Maximum Thermoluminescence Intensity

In this part of the study, the effects of the different waiting time in the dark on the maximum thermoluminescence intensity were investigated.

Figure 4.14 shows the variations of maximum thermoluminescence intensity as a function of waiting time in the dark environment for the (a) Turkcell sample, (b) Avea sample, and (c) Vodafone sample. In Figure 4.14 (a), the maximum

thermoluminescence intensity generally increases with increasing waiting time in the dark environment. Between and , the graph line is supralinear

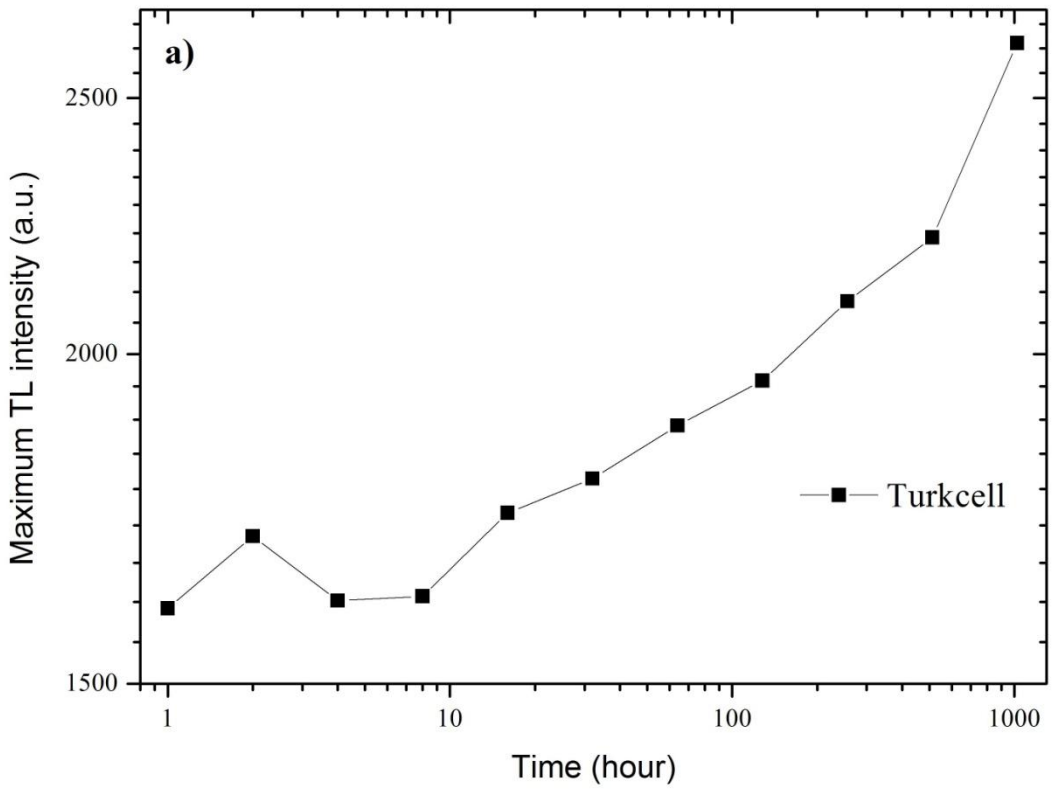

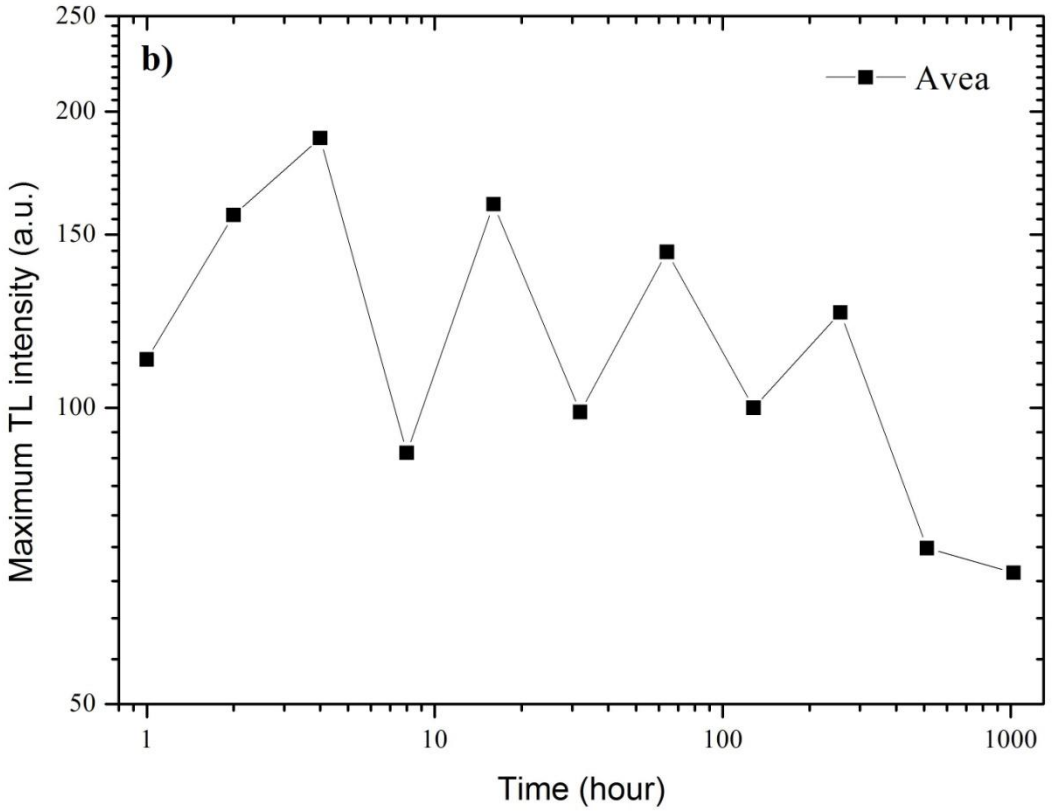

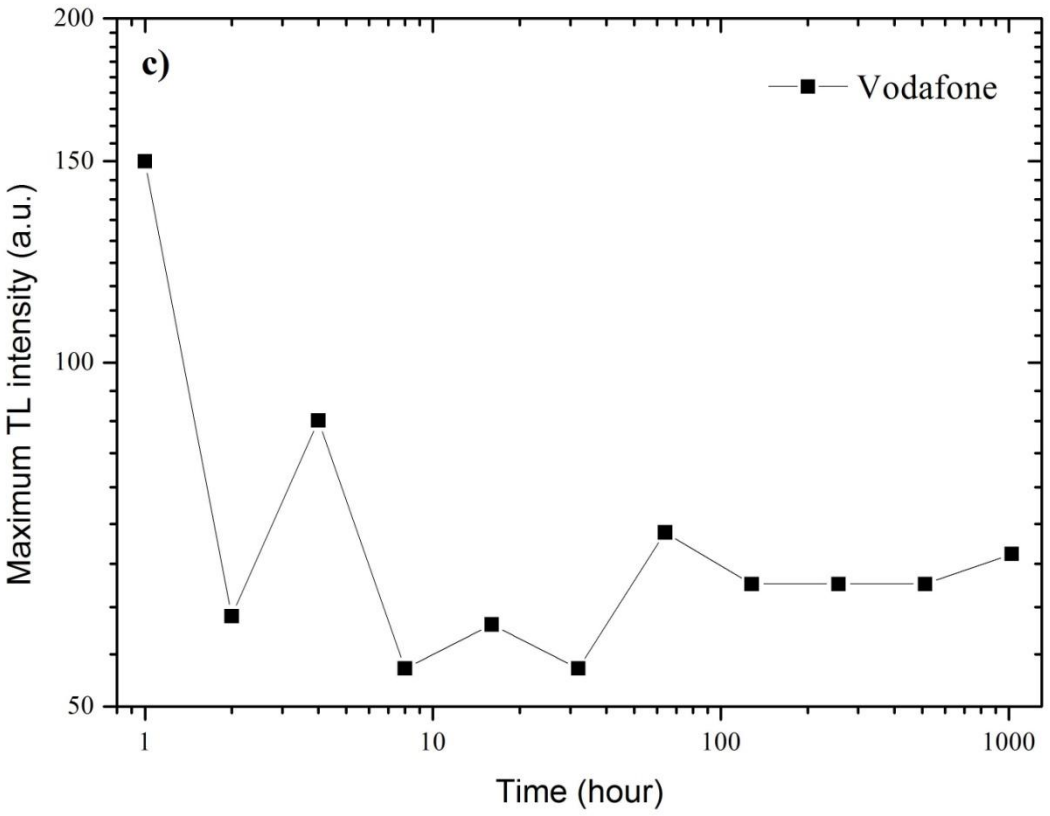

Figure 4.14 Variations of maximum thermoluminescence intensity for different waiting time in the dark for the (a) Turkcell sample, (b) Avea sample, (c) Vodafone sample.

except the waiting time. Between and , the graph line is linear. After , the graph line sharply increases with increasing waiting time. Turkcell SIM card chip has a good storage capacity and it shows the effects of radiation even past from radiation process. In Figure 4.14 (b), the maximum thermoluminescence intensity increases with increasing waiting time between and Between and , there are fluctuations and the maximum thermoluminescence intensity increases or decreases randomly with increasing waiting time. After , it begins to decrease with increasing waiting time. But the obtained glow curve is not good enough to make comments for Avea sample. In Figure 4.14 (c), there are lots of fluctuations. Between and the maximum thermoluminescence intensity increases or decreases randomly with increasing waiting time. Between and , the maximum thermoluminescence intensity remains constant with increasing waiting time. After , it begins to increase with increasing

waiting time. But the obtained glow curve is not good enough to make comments for Vodafone sample too.

4.4.4 Variation of Area Under Curve

In this part of the experiment, the effects of the different waiting time in the dark on the peak area were examined. Figure 4.15 shows the variations of area under curve as a function of waiting time in the dark for the (a) Turkcell sample, (b) Avea sample, and (c) Vodafone sample. In Figure 4.15 (a), the peak area generally increases with increasing waiting time in the dark. Between and , the graph line is supralinear except the waiting time. Between and , there are fluctuations and the peak area increases or decreases randomly. After it begins to increase with increasing waiting time in the dark. In Figure 4.15 (b), the peak area increases or decreases randomly. Between and the graph line is linear and the peak area increases with increasing waiting time. After , there is a decrement in the peak area. Between and , the graph line is linear and the peak area increases with increasing waiting time again.

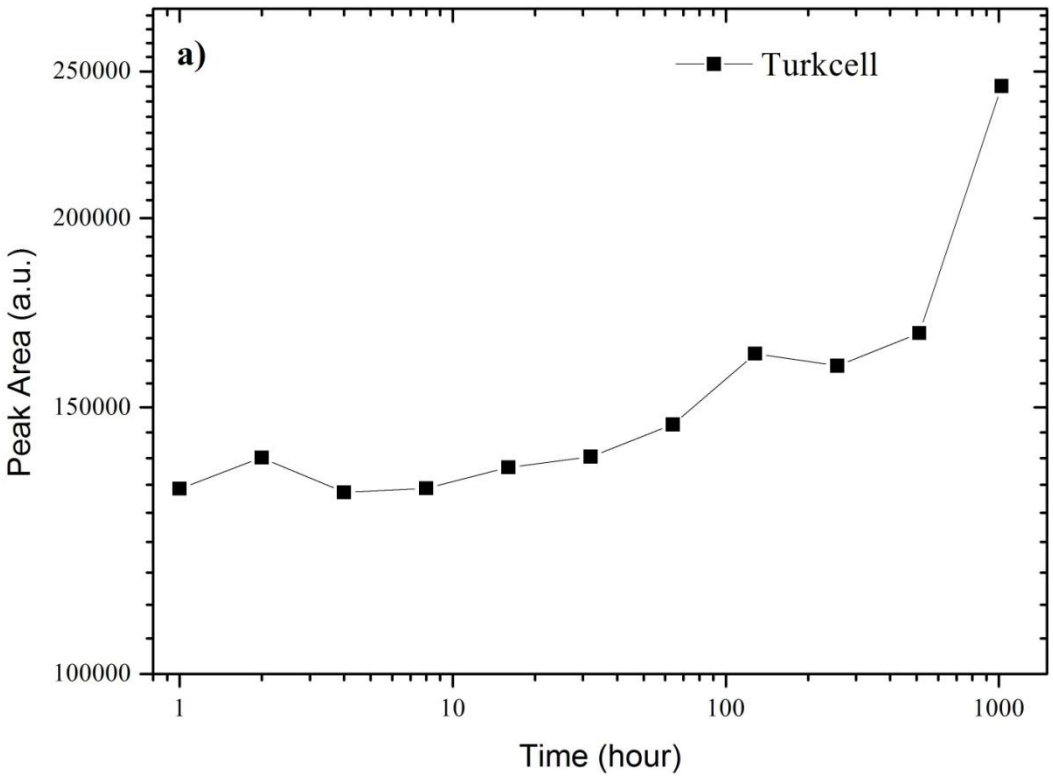

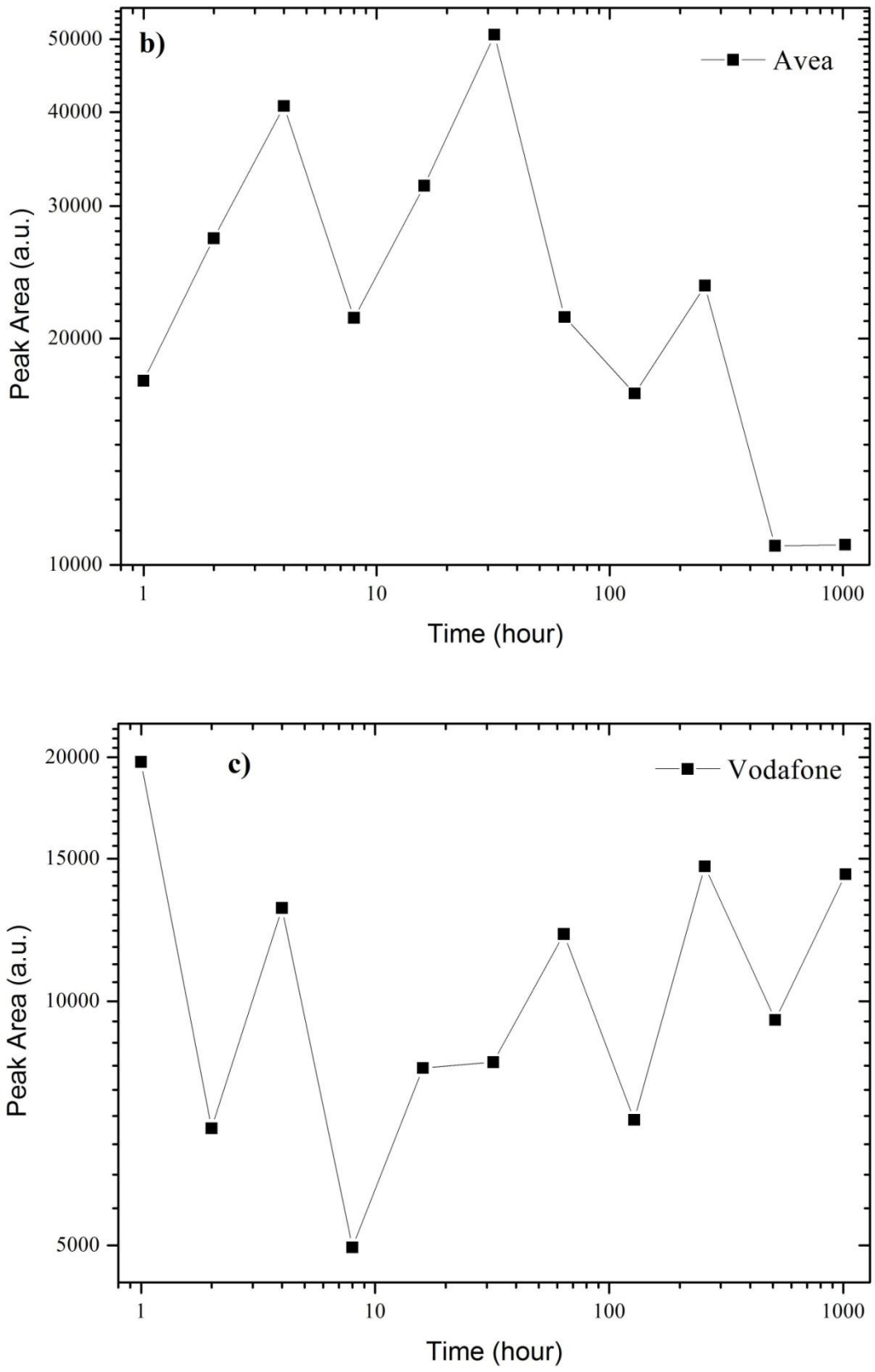

Figure 4.15 Area under curve for different waiting time in the dark for the (a) Turkcell sample, (b) Avea sample, (c) Vodafone sample.

Between and , the peak area sharply decreases with increasing waiting time. After there is a fluctuations. Between and the peak area remains constant. But the obtained glow curve is not good enough to make comments for Avea sample. In Figure 4. 15 (c), the peak area increases or decreases randomly. Between and and between and , there are fluctuations and the peak area increases or decreases randomly with increasing waiting time. Between and the peak area remains nearly constant with increasing waiting time. But the obtained glow curve is not good enough to make comments for Vodafone sample too.

CHAPTER 5
CONCLUSION

In our experiments, three main cases such as dose response, heating rate, cycle of measurements, and fading were studied.

In this study, Turkcell SIM card chip has a better results and better response to different dose values than Avea and Vodafone SIM card chips. Avea SIM card chip seems better than Vodafone SIM card chip too. The thermoluminescence intensity of Turkcell SIM card chip increases with increasing dose values so the Turkcell SIM card chip may used as a dosimeter. On the other hand thermoluminescence intensity of Avea and Vodafone SIM card chips randomly increase and decrease with increasing dose values so these SIM card chips are not useful as a dosimeter.

Heating rate experiments show that Turkcell SIM card chip has better results than Avea and Vodafone SIM card chips. The thermoluminescence intensity decreases and peak temperature of glow curve increases with increasing temperature increment for Turkcell SIM card chip. Avea and Vodafone SIM card chips increase or decrease randomly. The obtained glow curves from Avea and Vodafone SIM card chips are not good enough to make comments.

These experiments show that Turkcell has a repeatability property that it can be used many times for dosimetric applications. Because the results of dose response, normalized maximum thermoluminescence intensity and normalized area under curve are approximately same. On the other hand Avea has almost no results that are the same. Vodafone has nearly constant results for normalization of maximum thermoluminescence intensity but if we need to select the best chip for repeatability, then Turkcell is the only clear choice.

It is well known that the optical treatments highly affects the intensity of the thermoluminescence glow curves. Fading also affects the intensity of the thermoluminescence glow curves. The effects of waiting in the dark process on the thermoluminescence glow curves were observed for Turkcell, Avea, and Vodafone SIM card chips. Experiments show that Turkcell SIM card chip has a good storage capacity then Avea and Vodafone SIM card chips. Even past from radiation process Turkcell SIM card chip can show the effect of radiation.

In conclusion, all the SIM card chips that we used, have thermoluminescence properties. We can use the material in a Turkcell SIM card chip as a dosimeter. Additionally, that material can be used as a accidental dosimeter. Results of all the experiments show that the Turkcell SIM card chip material had the best response. The Avea SIM card chip has a better response than the Vodafone SIM card chip. However, more testing, using a larger number of samples, will be required in order to make a proper determination.

REFERENCES

[1] Bos, A. J. J. (2007). Theory of thermoluminescence. *Rad. Meas.* **41,** 45-56.

[2] McKeever, S. W. S. (1985). Thermoluminescence of solids. *Cambridge university Press.* Cambridge.

[3] Daniels F. and Boyd C. A. (1953). Thermoluminescence as a research tool. *Science,* **117**, 343-349.

[4] Aitken M. J., Tite M. S. and Reid J. (1964). Thermoluminescencent dating of ancient ceramics, *Nature,* **202**, 1032-1033.

[5] Aitken M. J., Zimerman D. W. and Fleming S. J. (1964). Thermoluminescencent dating of ancient pottery, *Nature,* **219**, 442-444.

[6] Mejdahl V. (1969). Thermoluminescence dating of ancient Danish ceramics. *Archaeometry*, **11**, 99-104.

[7] Wintle A. G. and Huntley D. J. (1985). Thermoluminescencent dating of ocean sediments. *Canadian journal of earth sciences.*

[8] Yahya H. and Thomas T. (2002). Smart card manufacturing. Munich: John Wiley & Sons, Ltd.

[9] H.Y. Goksu, I.K. Bailiff, V.B. Mikhailik, (2003) Radiat. Meas. 37, 323.

[10] R. Arik, (1992). Kubad-Abad Excavations (1980–1991), Anatolica 18, 101.

[11] Braunlich, P. (1983). *Thermally stimulated relaxation in solids*, Springer-Verlag.

[12] HalpBran A. (1985). Evaluation of thermal activation energies from glow curves, *Phys. Rev.*, **117**, 40.

[13] Wintle A. G. (1985). Anomalous fading of thermoluminescence in mineral samples, *Nature,* **245**, 143-144.

[14] Wintle A. G. (1985). Thermal quenching of thermoluminescence in quartz,*Geophys. J. R. Ast. Soc.*,**41**,107-113.

[15] Botter-Jensen L. (1997). Luminescence technique: instrumentation and methods. *Rad. Meas.*, **17**, 749-768.

[16] Randall J.T. and Wilkins M.H.F. (1945). Phosphorescence and Electron Traps. I. The Study of Trap Distributions. *Proc.R.Soc.London Ser. A* **184**, 366.

[17] Chen R. and McKeever S.W.S. (1997). *Theory of Thermoluminescence and Related Phenomena*, World Scientific, Singapore.

[18] Furetta, C. and Kitis G. (2004). Review of Thermoluminescence. *Journal of Materials Science.* **39**, 2277-2294.

[19] Garlick G.F.J. and Gibson A.F. (1948). The Electron Trap Mechanism of Luminescence in Sulphide and Silicate Phosphors. *Proc.Phys.Soc.* **60**, 574.

[20] May C.E. and Partridge J.A. (1964). Thermoluminescent kinetics of alpha;-irradiated alkali halides *J.Chem.Phys.* **40**, 1401.

[21] Kitis G., Gomez-Ros J.M. and Tuyn J.W.N. (1998). Thermoluminescence glow-curve deconvolution functions for first, second and general orders of kinetics *J.Phys.D:Appl.Phys.* **31**, 2636.

[22] Chen R. and Winer A.A. (1970). Effects of Various Heating Rates on Glow Curves. *J.Appl.Phys.* **41**, 5227.

[23] Piters T.M. and Bos A.J.J. (1993). A model for the influence of defect interactions during heating on thermoluminescence in LiF:Mg,Ti (TLD-100) *J.Phys.D:Appl.Phys.* **26**, 2255.

[24] Chen R (1969). On the Calculation of Activation Energies and Frequency Factors from Glow Curves *J.Appl.Physics* **40**, 570.

[25] Grossweiner L. I. (1953). A Note on the Analysis of First-Order Glow Curves *J.Appl.Physics* **24**, 1306.

[26] Bunghkbardt B., Singh D. and Piesch E. (1977). *Nuclear Instrumentations and Methods, **141,** 363.*

[27] Halperin A. and Braner A. A. (1960). Evaluation of Thermal Activation Energies from Glow Curves *Phys.Rev*. **117**, 408.

[28] Kathuria S. P. and Sunta C. M. (1979).Kinetics and Trapping Parameters TL in LiF TLD-100 *J.Phys.D:Appl.Phys.* **12**, 1573.

[29] Bos A. J. J., Piters J. M., Gomez Ros J. M. and Delgado A. (1993). Glacanin, and Intercomparision of Glow Curve Analysis Computer Programs IRI-CIEMAT Report, 131-93-005 IRI Delft.

[30] F.O. Ogundarea, F.A. Balogunb,and L.A. Hussaina.(2005) Heating rate effects on the thermoluminescence of fluorite, *ScienceDirect*, 40, 60-64.

[31] A. Mandowski, and A.J.J. Bos.(2011). Explanation of anomalous heating rate dependence of thermoluminescence in YPO4:Ce^{3+},Sm^{3+} based on the semi-localized transition (SLT) model, *Elsevier*, 46, 1376-1379.

[32] Munish Kumar, G.Chourasiya, B.C.Bhatt, C.M.Sunta. (2010). *Elsevier*, 130, 1216-1220.

[33] Reuven Chen,S. W. S. McKeever.1997. Theory of Thermoluminescence and Related Phenomena.Singapore:World Scientific.

[34] Claudio Furetta. (2008). Questions and Answers on Thermoluminescence (TL) and Optically Stimulated Luminescence (OSL).Singapore: World Scientific.

[35] M Oberhofer and A Scharmann. (1981). Applied thermoluminescence dosimetry. Luxembourg:Commission of the European Communities.

[36] Hüseyin Toktamis. (2008). Investigation of thermally stimulated luminescence characteristics of synthetic and natural quartz.

[37] David B Everett. (1992). Introduction to Smart Cards. Australia: *John Wiley & Sons, Ltd.*

[38] Claus Ebner.(2008). Smart card production environment, *Springer*, 38 , 27-50.

[39] MicroChemicals. (2001). http://www.microchemicals.eu/

[40] V. Correcher, J. Garcia-Guinea, and T. Rivera.(2009). Thermoluminescence sensitivity of daily-use materials, *Taylor & Francis Group*, 164, 232-239.

[41] H. Y. Goksu. (2003). Telephone chip-cards as individual dosemeters, *Pergamon*, 37, 617-620.

[42] I. Fiedler, C. Woda. (2011). Thermoluminescence of chip inductors from mobile phones for retrospective and accident dosimetry, *Elsevier*, 46, 1862-1865.

[43] Daniel Ekendahl, Libor Judas. (2012). Retrospective dosimetry wıth alumina substrate from electronic components, *Oxford Journals*, 150, 134-141.

[44] Thermo Scientific. (1956). http://www.thermoscientific.com/en/